DOI: 10.1002/chem.200800559

A Multilateral Mechanistic Study into Asymmetric Transfer Hydrogenation in Water

Xiaofeng Wu,[a] Jianke Liu,*[a] Devis Di Tommaso,[b] Jonathan A. Iggo,[a] C. Richard A. Catlow,[b] John Bacsa,[a] and Jianliang Xiao*[a]

Abstract: The mechanism of aqueous-phase asymmetric transfer hydrogenation (ATH) of acetophenone (acp) with HCOONa catalyzed by Ru-TsDPEN has been investigated by stoichiometric reactions, NMR probing, kinetic and isotope effect measurements, DFT modeling, and X-ray structure analysis. The chloride [RuCl(TsDPEN)(*p*-cymene)] (**1**), hydride [RuH(TsDPEN)(*p*-cymene)] (**3**), and the 16-electorn species [Ru(TsDPEN-H)(*p*-cymene)] (**4**) were shown to be involved in the aqueous ATH, with **1** being the precatalyst, and **3** as the active catalyst detectable by NMR in both stoichiometric and catalytic reactions. The formato complex [Ru(OCOH)(TsDPEN)(*p*-cymene)] (**2**) was not observed; its existence, however, was demonstrated by its reversible decarboxylation to form **3**. Both **1** and **3** were protonated under acidic conditions, leading to ring opening of the TsDPEN ligand. **4** reacted with water, affording a hydroxyl species. In a homogeneous DMF/H_2O solvent, the ATH was found to be first order in the concentration of catalyst and acp, and inhibited by CO_2. In conjunction with the NMR results, this suggests that hydrogen transfer to ketone is the rate-determining step. The addition of water stabilized the ruthenium catalyst and accelerated the ATH reaction; it does so by participating in the catalytic cycle. DFT calculations revealed that water hydrogen bonds to the ketone oxygen at the transition state of hydrogen transfer, lowering the energy barrier by about 4 kcal mol^{-1}. The calculations also suggested that the hydrogen transfer is more step-wise in nature rather than concerted. This is supported to some degree by the kinetic isotope effects, which were obscured by extensive H/D scrambling.

Keywords: asymmetric catalysis · hydrogenation · ruthenium · water

Introduction

Asymmetric transfer hydrogenation of ketones, as an efficient synthetic route to optically active alcohols, has attracted increasing attention in the last decade due to its great potential for applications in the fine chemical, pharmaceutical, agrochemical industries and in new materials.[1] Among the catalysts and ligands explored so far, the Noyori–Ikariya catalyst, that is, Ru-TsDPEN (TsDPEN = *N*-(*p*-toluenesulfonyl)-1,2-diphenylethylenediamine) [Eq. (1)],[2] has been mostly studied due to its high efficiency for ATH and structural versatility permitting further catalyst optimization [Eq. (1)].[3]

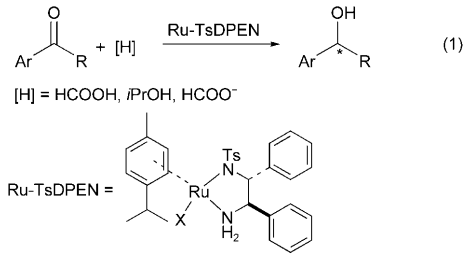

Continued ligand design based on the monosulfonylated diamine skeleton has improved catalytic productivity/enan-

[a] Dr. X. Wu, Dr. J. Liu, Dr. J. A. Iggo, Dr. J. Bacsa, Prof. J. Xiao
Department of Chemistry, University of Liverpool
Liverpool, L69 7ZD (UK)
Fax: (+44) 151 7943589
E-mail: j.xiao@liv.ac.uk

[b] Dr. D. Di Tommaso, Prof. C. R. A. Catlow
Davy Faraday Research Laboratory, Kathleen Lonsdale Building
University College of London, Gower Street
London, WC1E 6BT (UK)

Supporting information for this article is available on the WWW under http://www.chemeurj.org/ or from the author: Effects of formate, stirring speed, and solvents on ATH, DFT calculations, isotope exchange, NMR studies, catalyst stability, and X-ray crystallographic data.

tioselectivity and expanded the scope of substrates.[1,4] The reaction medium and hydrogen source employed are also crucial for the overall catalytic productivity. For example, higher yields and enantioselectivities were achieved by using formic acid/triethylamine azeotrope as both solvent and hydrogen source instead of isopropanol, where simultaneous loss of CO_2 and formation of ruthenium hydride through decarboxylation of formic acid drive the ATH reaction to completion.[3b] Recently we found that the ATH of aromatic ketones is significantly accelerated when the reaction is carried out in neat water with HCOONa as hydride donor.[5] Since then, a number of ATH reactions with various catalysts using formate in water have been reported.[6–8] These studies suggest that aqueous HCOONa is an ideal reductant for ATH reactions; the chemistry is made more appealing by the green character of water as a solvent and the safety and easiness of operation. Indeed, commercial applications of aqueous-phase ATH are already underway.[5e,9]

Our initial studies of ATH with Ru-TsDPEN revealed that not only does water accelerate the ATH rates, it enhances the life of the catalyst as well (also see the Discussion Section).[5a–c] Furthermore, the reduction rate and enantioselectivity were found to vary significantly with solution pH.[5c] The rate/pH dependence has been revealed for achiral transfer hydrogenation of carbonyl compounds with $[Ru(bipy)(\eta^6\text{-}C_6Me_6)(H_2O)]^{2+}$ (bipy = 2,2-bipyridine) and $[IrCp^*(bipy)(H_2O)]^{2+}$ ($Cp^* = \eta^5\text{-}C_5Me_5$),[10] and for a number of other chiral and achiral transfer hydrogenation catalysts.[1n,11] In closely related non-aqueous ATH reactions using formic acid as reductant from both industrial and academic laboratories, the ratio of $HCOOH/NEt_3$ has been shown to affect the ATH rate.[12] These observations prompted us to investigate the mechanism of aqueous-phase ATH reactions and the role of water in the catalytic cycle, in the hope that such insight would allow further improvement of this powerful, green transformation.

A great deal of progress has been made in mechanistic understanding of the transfer hydrogenation mechanism in organic solvents, which has been systematically reviewed.[1a,h–m] The Noyori–Ikariya Ru–TsDPEN catalytic system has received the most attention among a large number of catalysts employed for ATH of ketones and imines. For the reduction of ketones with Ru–TsDPEN in isopropanol, Noyori and co-workers proposed a concerted pathway for the hydrogen transfer process, that is, the hydridic hydrogen on Ru–H and the protonic hydrogen on the NH_2 moiety are transferred simultaneously to the carbon and oxygen atom of the carbonyl group, respectively (Scheme 1).[1a,3a,13] The intermediates depicted in Scheme 1 have been identified and characterized crystallographically.[3e] This concerted mechanism is also supported by kinetic isotope effect studies from Casey's group, which demonstrated a reversible, concurrent hydride and proton transfer from isopropanol to the 16-electron species in Scheme 1.[14] The same mechanism has also proven to work for the Shvo catalyst, which concurrently transfers its hydride on the ruthenium and proton on the OH moiety to the carbonyl group of ketone (Scheme 2).[15]

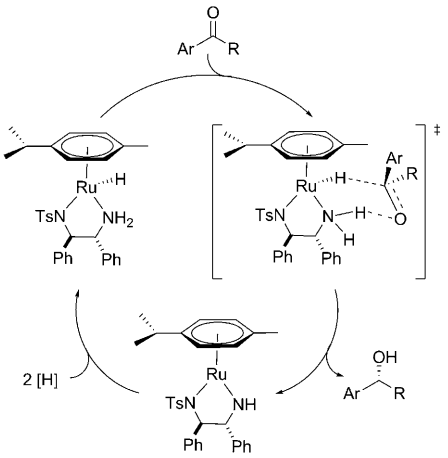

Scheme 1. Concerted hydrogen transfer mechanism for ATH of ketones catalyzed by Ru–TsDPEN catalyst.

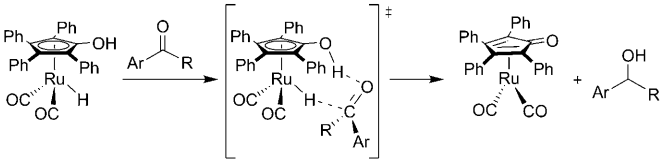

Scheme 2. Concerted hydrogen transfer mechanism for ATH of ketones catalyzed by the Shvo catalyst.

Although the concerted mechanism is widely accepted for ketone reduction in the above catalytic systems, a stepwise mechanism[16] has been proposed for a molybdocene hydride-catalyzed ketone reduction in water and isopropanol.[16a,b] In this mechanism, the ketone substrate is first bound to the molybdocene and then reduced to form a CpMo–alkoxide species, which is subsequently hydrolyzed to an alcohol. Another example of stepwise transfer hydrogenation of carbonyl compounds is seen in a ruthenium–acetamido complex; this is evidenced by an inverse deuterium isotope effect and competitive inhibition by added phosphines.[16c]

Besides the metal centers and auxiliary ligands, substrates can influence the reaction pathway. Thus, when using imines as a substrate, hydrogen transfer can follow either an outer-sphere pathway, similar to that proposed for carbonyl reduction (Schemes 1 and 2), or an inner-sphere mechanism in which imine coordination to the metal takes place prior to hydrogen transfer.[4d,17] Furthermore, in the Ru–TsDPEN-catalyzed ATH of imines reported by Bäckvall, yet another mechanism may come into play.[18] The ATH requires an acid to proceed;[18a] hence the reduction may proceed via the stepwise, ionic mechanism put forward by Norton[18b] and Bullock[18c] for hydrogenation reactions, which involves hydride transfer to a protonated imine as shown in Scheme 3. It is noted that the Ru–TsDPEN and Shov catalysts are active for both transfer hydrogenation and hydrogenation.[18d]

Despite the advances made on the mechanistic understanding of non-aqueous phase ATH reactions and the sig-

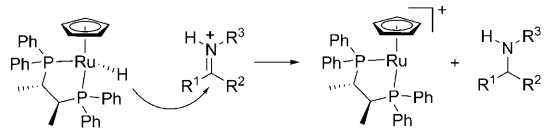

Scheme 3. Transfer hydrogenation of imines via an ionic mechanism.

nificant academic and commercial interest in the aqueous-phase ATH,[1n,9] a systematic study of the mechanism of ATH in water is not yet available. Given the various mechanistic pictures depicted above for the non-aqueous phase ATH and the polar, strong hydrogen-bonding nature of water, the following questions arise: Which mechanistic pathway is more likely in water? Is the same concerted mechanism still operative? Is water involved in the catalytic cycle? How does water accelerate and stabilize the catalyst, and why is the reaction pH-dependent? These questions are not straightforward to address, however. Firstly, characterization of the catalyst precursors and intermediates in water is relatively difficult due to the poor solubility of such complexes in aqueous solution. Secondly, most organic reactions in water are expected to experience diffusion control, resulting from the poor solubility of the substrates and catalysts or phase separation. These in turn hamper an accurate determination of the reaction kinetics.

In this work, a multilateral approach has been adopted to probe the mechanism of a benchmark aqueous-phase ATH [Eq. (2)] in order to shed light on the questions raised

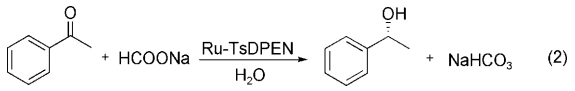

(2)

above. Specifically, we have performed detailed kinetic studies, including kinetic isotope effect measurements, of the reduction of acetophenone (acp) in a homogeneous dimethylformamide (DMF)/H_2O mixture. The aqueous DMF is chosen to minimize the effects of diffusion control, allowing the apparent aqueous-phase ATH kinetics to be determined for the first time; DMF is an innocent co-solvent in the ATH. The molecular structures and transformations of the ruthenium precatalyst, intermediates and hydrides under various conditions have been investigated by both NMR spectroscopy and X-ray crystallography. In addition, we have carried out DFT calculations in order to model the transition state of the hydrogen transfer step and map out the role of water. A very recent computational study of transfer hydrogenation in methanol has shown that methanol as solvent could lower the activation barrier of hydrogen transfer and even alter the mechanism.[19] Recently, there have also been several studies dealing with the effect of water on catalytic reactions;[6a,20] however, none is concerned with ATH reactions in water.

Results

Effects of reaction medium: Although excellent activities are achieved in the ATH of simple aromatic ketones in neat water, the poor solubility of substrates such as acp in water results in a biphasic reaction system, in which the Ru–TsDPEN catalyst resides mostly in the upper organic phase and the hydrogen donor (sodium formate in this study, see Table S1, Supporting Information; hereafter, all the tables, figures and schemes that appear in the Supporting Information are denoted with S) remains in the aqueous phase. This has severe implications for any kinetic study, since diffusion of reactants over the organic–water interface may dominate the kinetics, and this is indeed seen from the effect of agitation speed on the reduction rates (Figure S1). In order to examine possible co-solvent effects and establish a homogeneous ATH, a number of common organic solvents were therefore introduced and screened for the model reaction in Equation (2); the results are shown in Figure S2. As may be expected, the trend of initial reaction rate and average activity are approximately in line with the polarity of co-solvent, that is, DMF > CH_2Cl_2 > toluene > Et_2O > hexane, none of which, except DMF, is miscible in water. On the other hand, no effect on the *ee* was observed, which suggests that these co-solvents do not impact on the enantioselective step. The highest activities were achieved with mixtures of water and solvents such as DMF, methanol and ethanol. Alcohols were not further studied, however, due to their well-known ability to act as hydrogen donors. In all these studies, the Ru–TsDPEN catalyst was in situ generated from $[RuCl_2(p\text{-cymene})]_2$ and 2.4 equiv TsDPEN.

The miscibility of DMF and H_2O at arbitrary ratios allowed us to investigate systematically the impact of water content on the reaction in Equation (2) in mixtures of DMF/H_2O, while retaining a homogeneous liquid phase. As shown in Figure 1, approximate first-order kinetics over [acp] was observed with up to 80% (volume) water in the mixed solvents at 40°C. The solubility of the hydrogen source, sodium formate, increases with water content. Thus, the modest acceleration of the reaction rate from $k = 0.001\ min^{-1}$ in pure DMF to $k = 0.006$–$0.007\ min^{-1}$ on addition of 1 to 10% water is partly ascribed to the higher solubility of HCOONa in the aqueous mixture. However, the significant rate acceleration observed in solvent mixtures containing 20 to 80% water ($k = 0.05$–$0.18\ min^{-1}$) cannot simply be attributed to improved solubility of HCOONa, which fully dissolved when the water content was more than 10%. Rather, it suggests that bulk water has an accelerating effect on ATH, an effect that is challenging to explain but could result from the formation of a local hydrogen-bonding network, which enhances the hydrogen-bond donating capability of water and so the reaction rates.[20f] The reaction medium appeared slightly turbid when more than 80% water was added, although the rate acceleration was retained. Under this "heterogeneous" conditions, the local concentration of acp around the catalyst and the hydrogen-bonding capability of water may be enhanced,[20f] thus af-

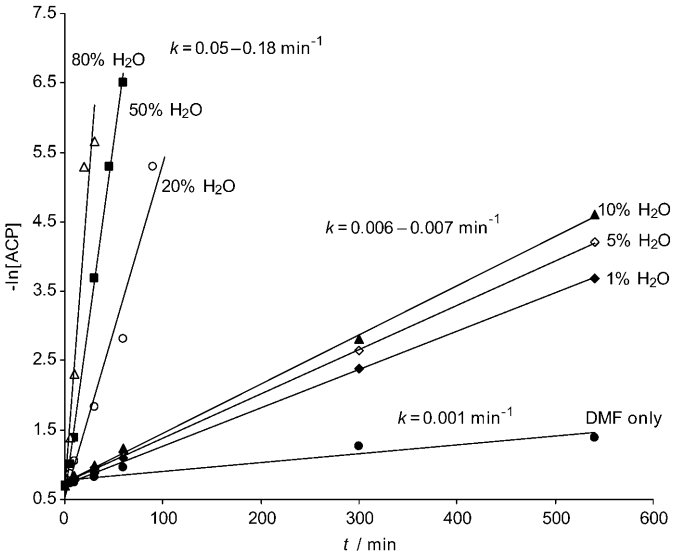

Figure 1. Plot of $-\ln[acp]$ vs reaction time for the ATH of acp in DMF/H_2O mixtures. The reactions were performed at 40 °C, with [Ru] = 4.7 mM, [substrate]/[catalyst] (S/C) = 100, [HCOONa]/[acp] = 5 in 2 mL solvents.

fording higher rates. On the basis of this study, a homogeneous DMF/H_2O (1:1, v/v) mixture was used as reaction medium for subsequent kinetic investigations.

Formation of Ru–TsDPEN catalyst in the presence of water: In our initial study, we assumed that the aqueous ATH proceeds via the catalytic cycle in Scheme 4 by analogy with Scheme 1. Noyori, Ikariya, and co-workers have synthesized, isolated and characterized catalyst precursor **1**, and active catalysts **3** and **4** (Scheme 4) in non-aqueous media.[3e] In isopropanol, a base is necessary to generate **1** from $[RuCl_2(p\text{-cymene})]_2$ and TsDPEN.

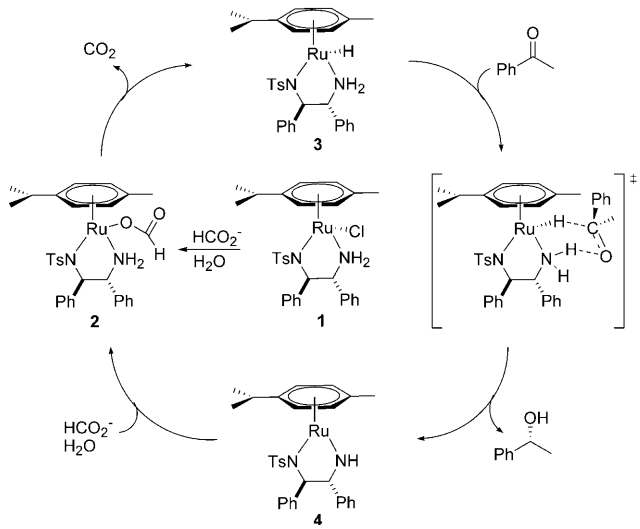

Scheme 4. Proposed mechanism for the ATH of acp with Ru–TsDPEN in water.

The formation of **1** in the presence of water was monitored by ^1H NMR spectroscopy. $[RuCl_2(p\text{-cymene})]_2$ and a stoichiometric amount of TsDPEN were stirred for 15 minutes at ambient temperature in a 1:1 (v/v) mixture of CD_2Cl_2 and D_2O, which was chosen to mimic the biphasic nature of the ATH reaction. ^1H NMR spectroscopy of the CD_2Cl_2 layer revealed the formation of **1**; a trace $[RuCl_2(p\text{-cymene})]_2$ was observed as the only species in the D_2O layer.

The same result was obtained for the reaction of $[RuCl_2(p\text{-cymene})]_2$ and 2.4 equiv TsDPEN in neat water at 40 °C followed by extraction with CH_2Cl_2. Both the NMR spectrum and molecular structure determined by X-ray crystallography are identical to those of compound **1** synthesized via Noyori's non-aqueous route.[3e] Apparently, water acts as the base in the aqueous preparation, facilitating the abstraction of HCl and the formation of **1**. Thus, the reaction solution became acidic upon formation of **1** (pH ≈2.8). However, our attempts to isolate a putative aquated Ru–TsDPEN complex, resulting from the substitution of Cl^- from **1** by H_2O, have been unsuccessful, although ruthenium–aqua complexes containing diamine ligands other than TsDPEN have recently been reported by several research groups.[7h,t,10a,21–24] In some instances, the aquation and anation equilibrium constants have been determined, and generally the formation of anation products is favored.[22,24]

On addition of 10 equiv HCOONa to **1** in the D_2O/CD_2Cl_2 mixture with stirring, the pale yellow water layer turned colorless immediately. ^1H NMR spectroscopy of the red orange CD_2Cl_2 layer confirmed the formation of the ruthenium hydride **3** (δ −5.80 ppm).[3e,25] In the aqueous phase, formate was observed as the dominant species (δ 8.40 ppm). Similarly, addition of excess HCOONa to **1** in neat water afforded **3** as a brick red solid. A transient orange coloration was observed during these reactions, indicating the presence of an intermediate formato complex **2**, which was rapidly transformed into the ruthenium hydride **3**. The instability of the formato complex is echoed by Ikariya's findings in THF; but he was able to isolate the corresponding acetate species.[26] When the same reaction was conducted in a closed reaction vessel, carbon dioxide and hydrogen were detected in the head space of the vessel by mass spectroscopy,[5c] suggesting that dehydrogenation of **3** to give **4** and the subsequent reactions to regenerate **3** take place in the absence of a ketonic substrate.

These results indicate that as with non-aqueous ATH, complexes **1–3** are formed in the corresponding aqueous reaction, with **1** being the precatalyst. Figure 2 shows the reaction profiles of **1** (in situ and preformed), **3**, and **4**, in the ATH of acp in DMF/H_2O. The insignificant difference in the reaction rates suggests that **3** and **4** are active catalysts in ATH in water and the formation of **1** and **3** is a fast process compared to transfer hydrogenation under the aqueous conditions. Taken together, the results show that essentially the same catalyst precursor and active catalytic species, as those reported previously for organic solvents, are involved in ATH in water.

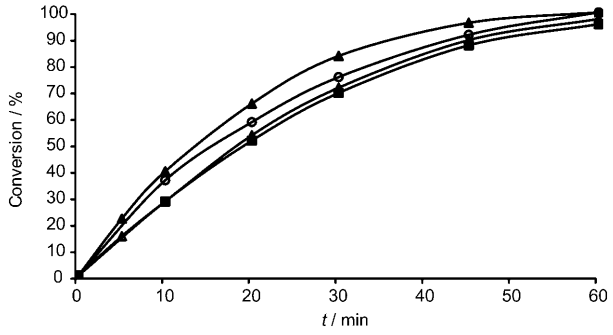

Figure 2. ATH of acp (1 mmol) with **1** (in situ, ▲; pre-formed, ■), **3** (○) and **4** (△) in DMF/H_2O 1:1 (2 mL) at a S/C ratio of 100, at 40 °C, using HCOONa (5 equiv) as hydrogen source.

Effect of water on the stoichiometric ATH of acp in CD_2Cl_2: With the availability of hydride **3**, the effect of water on hydride transfer to ketones could be directly examined. Figure 3 shows the progress of stoichiometric reduction

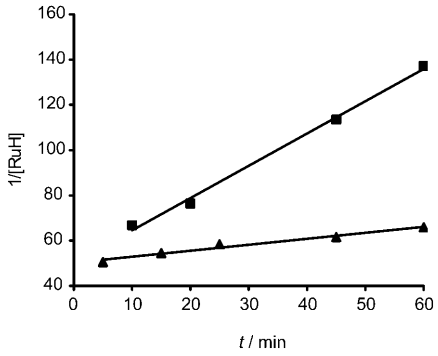

Figure 3. Stoichiometric reduction of acp with **3**: ▲ in dry CD_2Cl_2; ■ in wet CD_2Cl_2 (doped with 0.2% H_2O). The reaction was followed by ^1H NMR spectroscopy at 20 °C with initial [**3**] = [RuH] = 0.018 M.

of acp by **3** in dry and wet CD_2Cl_2 monitored by ^1H NMR spectroscopy, using ferrocene (δ 4.2 ppm) as internal standard. The concentration of the reactants and products were obtained by integrating the ^1H resonances at δ 2.6 (methyl group of acp), δ −5.8 (ruthenium hydride **3**), and δ 1.5 (methyl group of the phenylethanol product) against the internal standard. The kinetic profiles display an overall second-order kinetics on [RuH] (i.e., [**3**]) in this stoichiometric reaction, and hence are consistent with the rate = k-[acp][RuH] = k[RuH]^2, due to [RuH] = [acp]. The second order rate constant is $k = 0.004\ L\,mol^{-1}\,s^{-1}$ in dry CD_2Cl_2 but $0.024\ L\,mol^{-1}\,s^{-1}$ in wet (ca. 60 equiv H_2O with respect to **3**) CD_2Cl_2. The six-fold acceleration of the reaction rate on addition of trace water under otherwise identical conditions unambiguously demonstrates that water accelerates the ATH, and the acceleration stems at least partly from water being involved in the hydrogen-transfer step suggested in Scheme 4. This has been further addressed by a computational study (see below); but we need first to investigate the kinetics of catalytic ATH in order to determine if the ATH is limited by hydrogen transfer.

Kinetics of ATH in DMF/H_2O: Figure 4 shows the effect of the initial concentration of catalyst, substrate, and formate and the effect of CO_2 on the ATH of acp in DMF/H_2O (1:1, v/v). For those experiments carried out at constant [acp] = 0.47 M and varying [Ru] (2.4–9.5 mM), the rate constant shows a good linear relationship against the catalyst concentration (Figure 4a), from which a second-order reaction constant of $0.11\ L\,mol^{-1}\,s^{-1}$ is obtained. At constant [Ru] = 4.7 mM, the ATH reaction appears to show a first-order kinetics on the concentration of ketone over the range of [acp] = 0.2–1.3 M (Figure 4b), from which a second-order reaction rate constant of $0.11\ L\,mol^{-1}\,s^{-1}$ is obtained. This value is in agreement with the rate constant deduced from the rate dependence on the catalyst concentration. Under our standard reduction conditions, [acp] is ca 0.5 M. Variation of the concentration of sodium formate from 3 to 10 equivalents with respect to [acp] has only insignificant effect on the kinetic profile (Figure 4c). The same reactions were repeated, adding $NaBF_4$ to adjust the molar ratios of salts versus substrate to 10:1 for all reactions. Again, no clear correlation between the reaction rates and [HCOONa] could be established, eliminating a possible effect of ionic strength on the rate. Thus, the overall reaction shows a first-order kinetic dependence on both [Ru] and [acp].

However, decreasing reaction rates were observed at higher acp concentrations (> 1.3 M) (Figure 4b). This could arise from substrate inhibition; no phase separation was observed under these reaction conditions (Figure 4b). The substrate inhibition could result from possible destruction of the hydrogen-bonding network of water[20f] and/or deprotonation of the ketone by the 16-electron **4** as found by Ikariya.[27] A similar phenomenon was reported recently by Noyori et al. for the asymmetric hydrogenation of acp catalyzed with [Ru(OTf)(TsDPEN)(*p*-cymene)] (OTf = $CF_3SO_3^-$) under slightly acidic conditions.[28] Substrate inhibition on related reactions has been discussed and summarized by de Vries very recently.[27b]

CO_2 is formed during the catalysis, which has an inhibition effect also shown in Figure 4d. Thus, switching the headspace gas from N_2 to CO_2, 10 min after the reaction started, significantly suppressed the ATH reaction. When the gas switching was done in the reverse order, that is, from CO_2 to nitrogen, a long induction period was observed before the reaction rate recovered. The results suggest that CO_2 inhibits the ATH reversibly, and this likely results from the decarboxylation of **2** to generate **3** being reversible (Scheme 4).[29] The fast decay in the reaction rate upon introduction of CO_2 probably results from the high reactivity of Ru–H towards CO_2, as similar ruthenium complexes are known as catalysts for hydrogenation of CO_2 (see below). Under normal catalytic conditions, however, CO_2 is reacted with OH^- to form bicarbonate and so will not impact significantly on the reduction rate. The sluggish recovery of the

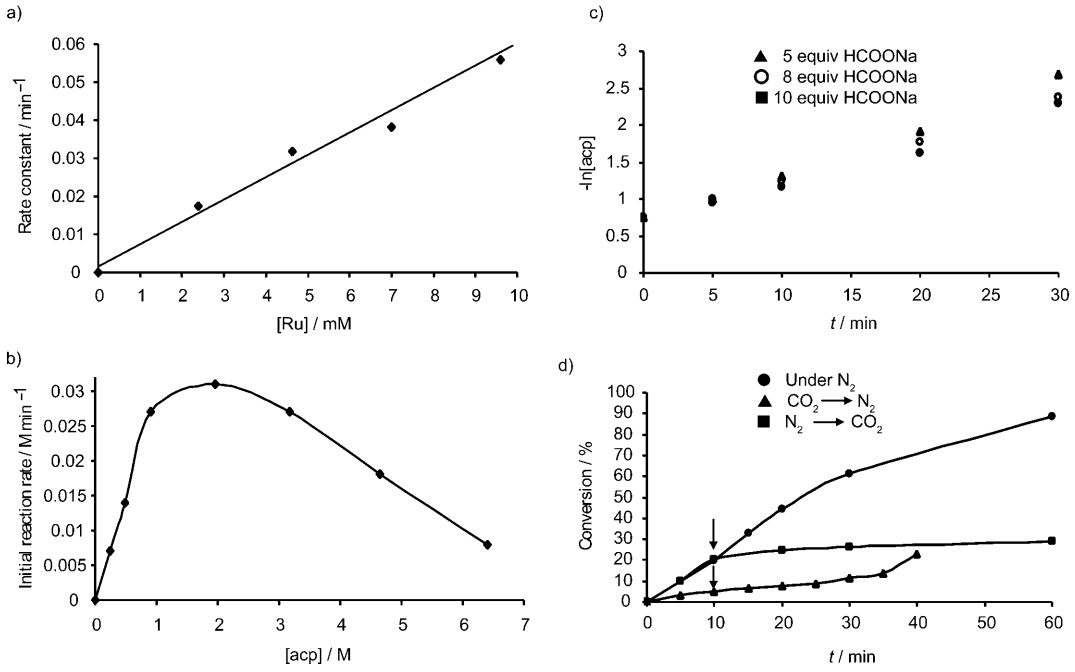

Figure 4. Kinetics of ATH of acp in DMF/H_2O 1:1 at 40 °C with [Ru] = 4.7 mM, S/C = 100, [HCOONa]/[acp] = 5 unless otherwise indicated: a) Effect of the concentration of catalyst on the rate constant measured from initial rates. b) Effect of the initial concentration of substrate on the initial rate. c) Effect of [HCOONa] (equivalents relative to acp). d) Effect of CO_2 (gas in the head space was switched 10 min after the reaction started).

catalyst activity on purging with N_2 may reflect the dehydration of H_2CO_3 being a slow process.[30]

A rate law consistent with the above results is given in Scheme 5, assuming that the coordination of formate and decarboxylation are reversible and equilibrated prior to hydrogen transfer.[31] When using HCOONa as reductant in water, the initial solution is approximately pH neutral and with the progress of ATH, the pH increases to about 9 under normal aqueous conditions.[1n,5c] Thus, the term $[CO_2][OH^-]$ is expected to be small as the CO_2 would be trapped as bicarbonate following the decarboxylation of **2** as aforementioned. Therefore, the rate law may be further reduced to a simple second-order kinetics over the concentration of catalyst and substrate as observed. The kinetic studies are thus consistent with the ATH in water being rate-limited by the hydrogen-transfer step, presumably with a transition state as suggested in Scheme 4. Under more basic conditions, however, the ATH will be slower, as has already been observed experimentally.[5ci,32]

Figure 5 presents an Eyring plot for the ATH of acp in the DMF/H_2O mixture over the temperature range of 20 to 80 °C, from which an activation enthalpy of 12.8 kcal mol^{-1} and activation entropy of −25.0 cal K^{-1} mol^{-1} were obtained. These values can be compared with those measured by Casey for dehydrogenation of isopropanol to give acetone by complex **4** ($\Delta H^{\neq} = 5.8$ kcal mol^{-1}, $\Delta S^{\neq} = -48.0$ cal K^{-1} mol^{-1}), which is the rate-determining step for ATH when isopropanol is the hydrogen donor.[14] In a more relevant study, Ikariya has measured the activation parameters of $\Delta H^{\neq} = 18.2$ kcal mol^{-1} and $\Delta S^{\neq} = -9.0$ cal K^{-1} mol^{-1}

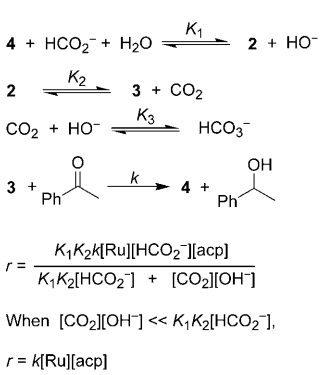

Scheme 5. Suggested rate law for the aqueous ATH of acp, where [Ru] refers to the total concentration of catalyst.

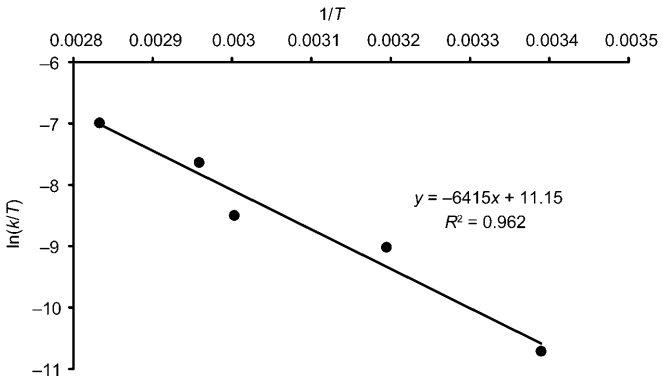

Figure 5. Eyring plot for the ATH of acp at various temperatures under otherwise identical conditions to those described in Figure 4.

for the decarboxylation of formic acid from **2** in [D_8]THF.[26] It is surprising that the activation enthalpy for the individual decarboxylation reaction is larger than that of the whole ATH reaction of acp (18.2 vs 12.8 kcal mol^{-1}). This suggests that the activation barrier of decarboxylation of the ruthenium formato intermediate is significantly reduced when the reaction is carried out in water. The large negative activation entropy of -25.0 cal K^{-1} mol^{-1} indicates that a well ordered transition state is likely to be involved; this appears to be consistent with Scheme 4.

Kinetic isotope effects: The NMR and kinetic studies described above agree with the rate of the aqueous ATH being limited by the hydrogen transfer step, and the kinetics further suggests that the hydrogen transfer may proceed via the metal–ligand bifunctional mechanism proposed for non-aqueous ATH (Schemes 1 and 4).[1k,n,13b,33] This mechanism implies a concerted transfer of the hydride and proton onto the ketone. To gain more evidence, we investigated the kinetic isotope effects (KIE) in the ATH of acp. Casey and Bäckvall have used KIE to study related hydrogenation and transfer hydrogenation reactions in organic media.[14,15] In their studies, isopropanol was used as hydrogen source to offer both H^+ and H^- for the transfer hydrogenation. Their studies support a concerted transfer of hydride and proton from Ru–TsDPEN to ketone. In our aqueous catalytic system, the reaction is carried out under neutral to basic conditions, thus $HCOO^-$ acts as hydride donor, and H_2O acts as the proton donor. Table 1 presents the rate constants, calculated from the initial reaction rates, for the ATH of acp using isotopically labeled DCOONa and/or D_2O performed in the 1:1 homogeneous DMF/H_2O mixture or the isotopically labeled mixture.

Table 1. Kinetic isotope effects of ATH of acp.[a]

Isotope used	k_H/k_D[b]
HCOONa/H_2O/DMF	1
HCOONa/H_2O/[D_7]DMF	1.06 ± 0.10 ($k_{DMF}/k_{[D_7]DMF}$)
HCOONa/D_2O/DMF	1.68 ± 0.10 (k_{RuHNH}/k_{RuHND})
DCOONa/H_2O/DMF	2.24 ± 0.10 (k_{RuHNH}/k_{RuDNH})
DCOONa/D_2O/DMF	3.05 ± 0.50 (k_{RuHNH}/k_{RuDND})
DCOONa/D_2O/[D_7]DMF	3.10 ± 0.50 (k_{RuHNH}/k_{RuDND})

[a] Conditions: 1 mmol acp, 5 equiv formate, in 2 mL solvent (DMF/H_2O 1:1) at 40 °C, S/C = 100. [b] Determined from the initial reaction rates, assuming DOONa leads to Ru–D and D_2O to Ru–ND_2.

An insignificant KIE was observed for DMF versus [D_7]DMF ($k_{DMF}/k_{[D_7]DMF} = 1.06$), consistent with DMF acting solely as co-solvent. The observed KIE, $k_{RuHNH}/k_{RuHND} = 1.68$ when using D_2O, and $k_{RuHNH}/k_{RuDNH} = 2.24$ when using DCOONa, is similar to those observed by Casey for stoichiometric hydrogen transfer from [RuH(TsDPEN)-(*p*-cymene)] to acetone, where $k_{RuHNH}/k_{RuHND} = 1.69$ and $k_{RuHNH}/k_{RuDNH} = 2.46$, which were attributed to arising from Noyori's concerted mechanism.[14,15b,c,34] Our results thus appear to be consistent with the hydrogen transfer to acp as the rate-determining step in the aqueous ATH. However, for a single-step, concerted hydrogen transfer process, the product of the individual isotope effects should be equal to the isotope effects of the double-labeled reactants. In our case, however, $k_{RuHNH}/k_{RuHND} \times k_{RuHNH}/k_{RuDNH} = 3.76$, which deviates significantly from the measured $k_{RuHNH}/k_{RuDND} = 3.05$ when using DCOONa/D_2O as hydrogen source. Whilst this partly arises from the Ru–TsDPEN-catalyzed scrambling of the deuterium label between water and formate (Figure S3 in the Supporting Information), complicating the interpretation of KIE in this system, our DFT calculations to be described below suggest that the hydrogen transfer in water is actually not entirely concerted.

DFT calculations: The results presented thus far are consistent with the Ru–TsDPEN-catalyzed ATH of acp in water proceeding via the pathways shown in Scheme 4, with the rate possibly being determined by the hydride transfer from the metal center to ketone. They cannot answer, however, why the ATH is faster in the presence of water. To shed light on this issue, density functional theory (DFT) calculations were performed. Previous ab initio and DFT calculations on model gas-phase complexes have shown that Noyori's concerted transfer of the hydridic Ru–H and the protic N–H to the ketone C=O linkage (**TS-A**, Scheme 6) is energetically favorable over other mechanisms proposed in the literature.[1j,k,m,n,13,35] However, those studies did not explicitly incorporate the effect of solvent molecules. Very recently, a DFT-based molecular dynamics study on a model [RuH-(aminoalcohol)(η^6-benzene)] complex has revealed that methanol solvent molecules hydrogen bond to the substrate formaldehyde, lowering the transition barrier of the reduction and rendering the hydrogen transfer "sequential" instead of concerted.[19]

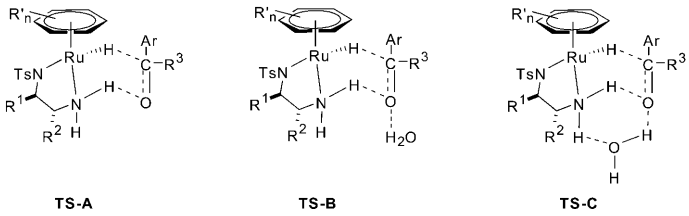

Scheme 6. Proposed transition states with and without participation of water molecule.

In order to probe the possible effect of water on the hydrogen transfer step, we considered two possible variations to the classical six-membered transition state structure, namely **TS-B** and **TS-C** (Scheme 6). In **TS-B**, a water molecule mediates the hydrogen transfer process through the formation of a hydrogen bond with the oxygen atom of the carbonyl functionality, whereas in **TS-C** the water molecule forms a bridging hydrogen bond between the amine and carbonyl groups. In the DFT calculations, we considered a simplified model hydrogen transfer, in which [RuH($NH_2CH_2CH_2NH$)(η^6-benzene)] (**5**) reacts with acetone as the hydrogen acceptor. The structures corresponding

to **TS-A** and **TS-B** were fully optimized and the saddle point characters of the optimized structures were verified by evaluation of the harmonically vibrational frequencies. However, it was not possible to locate a transition state structure corresponding to **TS-C**; hence **TS-C** was considered unlikely.[36]

Schemes 7 and 8 illustrate the structures present in the reaction pathway associated with the transition states **TS-A** (**7**) and **TS-B** (**10**), respectively. The relative energies of the intermediates, transition states and products are given in the Supporting Information (Tables S2 and S3). Lower activation energies are predicted by the BLYP versus the BB1K method in line with the well known tendency of pure DFT methods to systematically underestimate reaction barriers.[37] The computed forward activation energy (ΔE^{a}, **6** → **7**) for the hydrogen transfer to acetone from **5** is 13.8 kcal mol^{-1} at the BB1K level (BLYP, 10.5 kcal mol^{-1}) for the pathway involving **TS-A** (Scheme 7).

Both DFT methods reveal a significant lowering of the activation energy when a water molecule mediates the hydrogen transfer process, with the forward activation energy (ΔE^{a}, **9** → **10**) computed at BB1K level being 9.3 kcal mol^{-1} (BLYP, 7.0 kcal mol^{-1}) (Scheme 8). Moreover, the reaction pathway associated with the transition state **TS-B** (**10**) is considerably more exothermic than the reaction involving **TS-A** (**7**). The results of the DFT-BLYP calculations are summarized in Scheme 9.

A comparison of the internuclear distances of the transition states indicates that **TS-B** is more similar to the reactants than **TS-A**. Thus, difference in the calculated Ru–H distance in **9** (1.630 Å) and **10** (1.744 Å) is much smaller than that in **6** (1.627 Å) and **7** (2.006 Å). Similarly, the out-of-plane angle (where the plane is defined by the oxygen and the carbons of the two methyl groups in the acetone) of the carbonyl carbon is 29.6° in **7** but only 21.2°

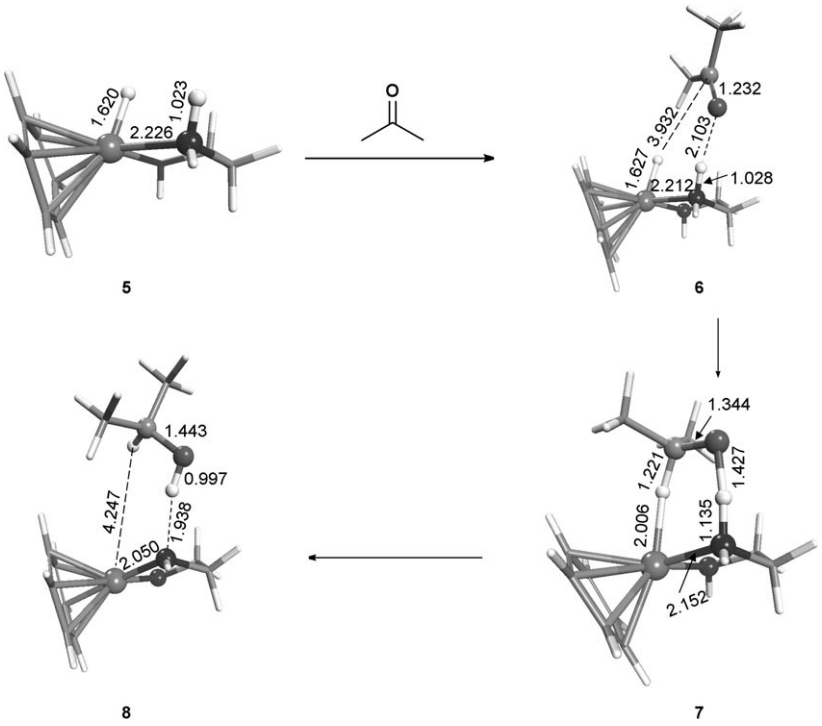

Scheme 7. DFT modeling of transfer hydrogenation of acetone by a model hydride [RuH($NH_2CH_2CH_2NH$)(η^6-benzene)] (**5**) (distance in Å).

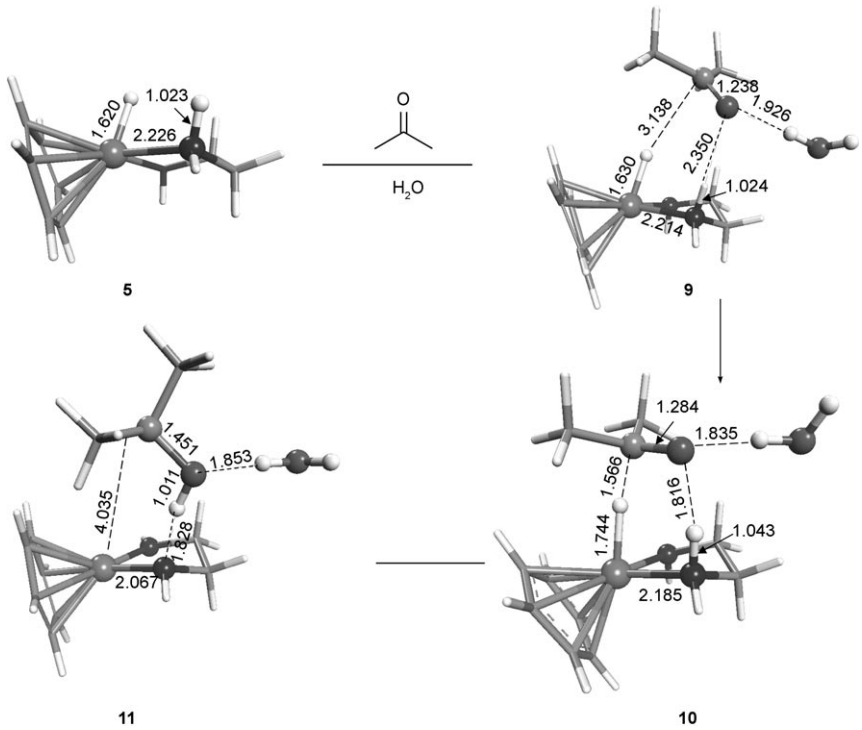

Scheme 8. DFT modeling of transfer hydrogenation of acetone by a model hydride **5** in the presence of a H_2O molecule (distance in Å).

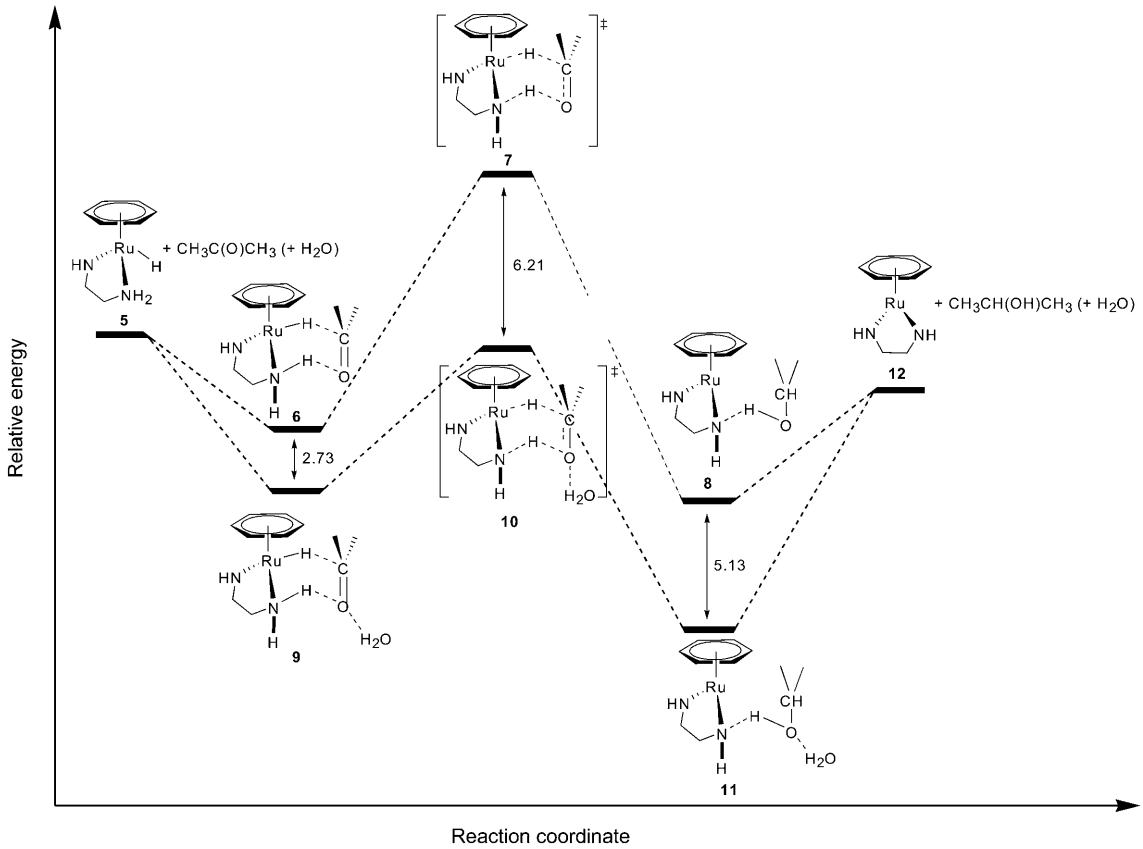

Scheme 9. Energy profiles for transfer hydrogenation of acetone calculated by the DFT BLYP method (energy difference in kcal mol^{-1}).

in **10**. The same trend is also evident in the other calculated internuclear distances. This is in line with the Hammond principle, that is, the higher exothermicity in the presence of water renders **TS-B** resembles the reactants more than **TS-A** does.

Scheme 10 shows the isosurface of the Kohn–Sham wave functions corresponding to the highest HOMO of **TS-A** and **TS-B** and to the HOMO−2 of **TS-B**. In the HOMO of both **TS-A** and **TS-B**, the *s* orbital of the electronegative hydride has bonding interaction with the vacant *p* orbital of the carbonyl carbon, while the Ru–H bond itself possesses an anti-bonding character. On the other hand, in the N···H···O region, the hydrogen atom is placed exactly at the node between the two phases of the wave function (this can be better seen in Scheme S1, where the threshold for the regions of constant electron density ρ has been decreased to $\rho = \pm 0.0016$ Å^{-3}), which corresponds to a typical HOMO shape for hydrogen-bonded species. However, the electron-charge density along the N···H···O linkage is considerably higher in the case of **TS-A** than that computed for **TS-B**, meaning that the hydrogen bonding interaction between the N-H and O atoms is smaller in **TS-B** than in **TS-A**. Scheme 10 also shows the HOMO-2 of **TS-B**, demonstrating the existence of a stronger hydrogen-bonding interaction between (C=O)···H_{water} than (C=O)···H···N.

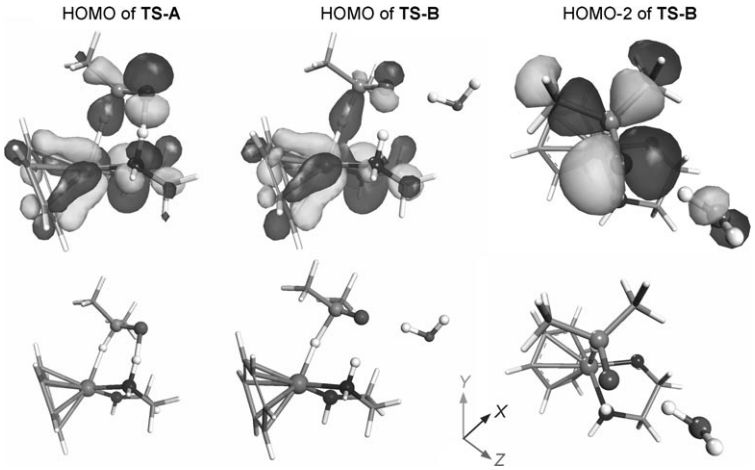

Scheme 10. HOMO of **TS-A** and **TS-B**, and HOMO−2 of **TS-B**. Different colors are used to identify the phase of the wave functions. Surfaces represent regions of constant electron density of $\rho = \pm 0.03$ Å^{-3}.

Further insight into the transition state was obtained by vibrational analysis of the transition state structures. For **7** (**TS-A**), the single imaginary frequency (134i cm^{-1}) is largest at the N···H···O linkage and second largest at Ru···H···C, indicating that cleavage of these bonds occurs synchronously. However, the single negative frequency of **10** (**TS-B**) (303i cm^{-1}) corresponds mostly to the transfer of the hydride between Ru and the carbonyl C atom, and less extensively to the proton transfer between the N and O atoms, suggesting again that the hydride and proton transfer is not entirely concerted in **TS-B**. This alteration in the mode of hydrogen transfer may have also contributed to the experimentally observed KIE presented above, and is in line with the findings on the formaldehyde reduction aforementioned.[19]

Effect of solution pH on catalytic species: Having established the aqueous-phase reaction kinetics and mechanism under neutral conditions, we turned attention to how the species in Scheme 4 would be affected by water and solution pH. Our previous studies showed that ATH of acp in water by Ru–TsDPEN is retarded at high pH, whilst both the reaction rate and ee decrease under acidic conditions, which we attributed to protonation of the amide nitrogen of TsDPEN and the resulting ring opening of the chelated ligand.[5c] The effect of pH on ATH has also been noted by other groups.[7e,g,h,s,8e] Furthermore, Noyori et al have recently reported that the triflate analogue of **1** is an efficient catalyst for asymmetric hydrogenation under slightly acidic conditions.[18d,27,38] Thus, the structure and configuration of the Ru–TsDPEN catalyst may well be pH dependent. However, no spectroscopic studies of how pH affects catalyst structures are available. We have therefore used NMR spectroscopy to study changes in the species present and their coordination chemistry.

Neutral conditions: The ATH in water is most efficient around the neutral conditions;[5,12d] hence, we first attempted to investigate the aqueous chemistry of the active species **3** and **4** under such conditions. The coordinatively saturated **3** is only sparingly soluble in water, suggesting that its solvation by water may be insignificant. In contrast, the 16-electron species **4** is partially soluble in water, and therefore is likely to interact with water molecules. To facilitate the NMR measurements, however, wet CD_2Cl_2 was used as solvent. On addition of trace water, two new resonances at $\delta = 10.0$ and 1.7 ppm were seen in the ^1H NMR spectrum of freshly prepared CD_2Cl_2 solution of **4** recorded at 20 °C. A third broad singlet was observed at δ −1.0 in the ^1H NMR spectrum at −80 °C (Figure S4). The intensities of these three resonances were significantly reduced on addition of D_2O (Figure S5), and they are thus tentatively assigned to a ruthenium aqua **13** and hydroxide complex **14** (Scheme 11). The resonance at $\delta = 1.7$ ppm can be assigned to the coordinated water molecule in the ruthenium aqua complex **13** by analogy to similar complexes reported by Makihara et al.[39] The resonance at $\delta = -1.0$ ppm is ascribed to the Ru-OH.[9] The resonance at $\delta = 10.0$ was only detected under carefully controlled conditions, and thus is attributed to the acidic NH protons, which undergo fast exchange with "free" water molecules.

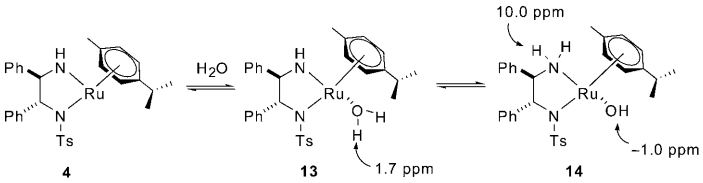

Scheme 11. Reaction of **4** and water.

Acidic conditions: When the Ru–TsDPEN-catalyzed ATH is performed under acidic conditions, for example, use of the azeotropic formic acid/triethylamine mixture as hydrogen donor, the reduction is sluggish.[5c,12d] We previously suggested that this is a result of TsDPEN dissociation from Ru^{II} caused by protonation.[5c] We have now probed the structure of **3** in the presence of an acid, and to facilitate interpretation, we introduced a spectator ligand, bis(diphenylphosphino)ethane (DPPE), the coordination chemistry of which in related compounds is well-known.[40] It is noted that DPPE does not inhibit the ATH by Ru–TsDPEN under neutral conditions.[5c,12d]

Following addition of one equivalent DPPE to a CD_2Cl_2 solution of **3** at −30 °C, the $^{31}P\{^1H\}$ NMR spectrum was dominated by the resonance of free DPPE at δ_P −13.0 (Figure 6a), showing no reaction with **3**. On subsequent addition of about 2 equiv CF_3SO_3H in aliquots, two pairs of doublet resonances, at δ_P 32.9 and −13.2 ppm with $J(PP) = 33$ Hz, and at δ_P 75.0 and 70.5 with $J(PP) = 30$ Hz, and a broad resonance at δ_P 9.2 were observed (Figure 6b). The first pair of resonances is attributed to complex **15** on the basis of the

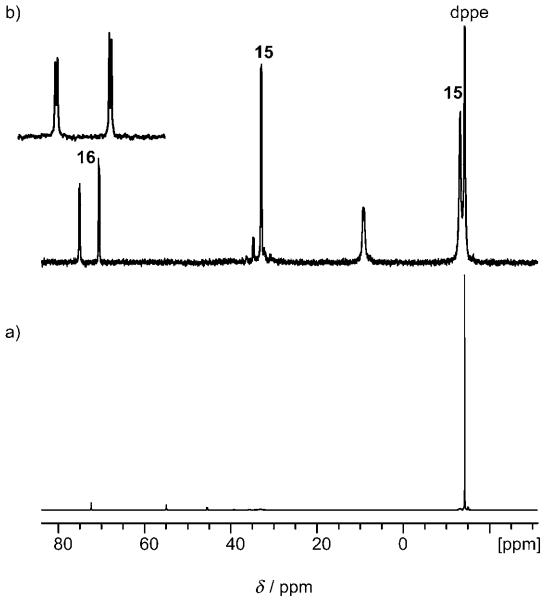

Figure 6. $^{31}P\{^1H\}$ NMR spectra of **3** + DPPE in a) CD_2Cl_2 and of the same on addition of b) CF_3SO_3H at −30 °C.

chemical shifts, which clearly indicate a dangling DPPE ligand (Scheme 12). The second pair of doublets arises from **16**, which has been recrystallized from a CD_2Cl_2 solution and characterized by both NMR spectroscopy (Figures S6–S8) and X-ray crystallography (Figure 7). The broad resonance at $\delta_P = 9.2$ is due to the protonated DPPE ligand,[41] which results from the decomposition of **15** or **16** under the acidic conditions. The formation of **15** and **16** is presumably accompanied with release of hydrogen.[10d] As aforementioned, hydrogen was detected when **1** was treated with HCOONa in water in the absence of acp.

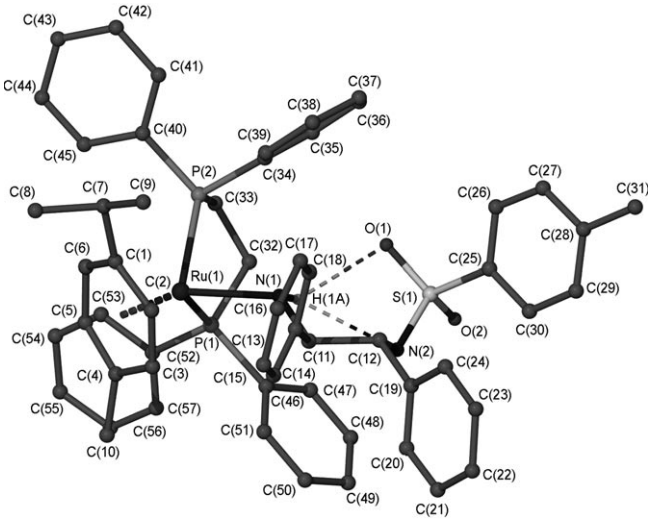

Figure 7. Molecular structure of **16** in $[\mathbf{16}][CF_3SO_3]_2 \cdot CH_2Cl_2$ in the solid state. The anions and solvent molecules are omitted for clarity. Selected distances [Å] and bond angles [°]: Ru(1)–N(1) 2.215(4), Ru(1)–P(1) 2.3176(16), Ru(1)–P(2) 2.3443(16), N(1)–H(1A) 0.88(5), N(1)···O(1) 3.043(6), N(1)···N(2) 2.919(6), P(1)-Ru(1)-P(2) 82.85(6), N(1)-Ru(1)-P(1) 85.12(15), N(1)-Ru(1)-P(2) 88.05(13). N(1)-H(1A)···O(1) 128(5), N(1)-H(1A)···N(2) 115(4).

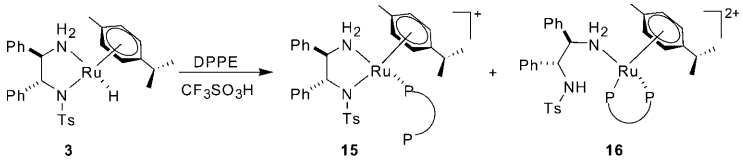

Scheme 12. Protonation of **3** in the presence of DPPE.

The isolation of **16** confirms our earlier suggestion that the coordinated TsDPEN can be protonated and the protonation occurs at the amindo nitrogen.[5c] As is shown in Figure 7, the Ru center in compound **16** has a distorted octahedral environment constituted of the η^6-cymene, chelated DPPE, and the amino group of TsDPEN. The N(1)···O(1) and N(1)···N(2) distances of 3.043 and 2.919 Å, respectively, indicate the presence of a moderate three-centered hydrogen bonding through H(1A). The slightly elongated Ru(1)–N(1) distance (2.215 Å) (cf. 2.117 Å in **1** and 2.110 Å in **3**[3e]) can be ascribed to the electron donating and sterically demanding properties of the coordinated DPPE. The difference in the Ru–P bond lengths, Ru(1)–P(1) = 2.318 Å and Ru(1)–P(2) = 2.344 Å, confirms that the inequivalence of the two phosphorus atoms is retained in the solid state, which results from the proximity of the chiral ligand. Thus, selective protonation of the amido nitrogen of TsDPEN under acidic conditions has unambiguously been demonstrated for the first time. As aforesaid, this ring opening leads to reduced catalyst activity and enantioselectivity, although other possible explanations cannot be ruled out.

Bearing in mind that when the precatalyst is generated in situ from $[RuCl_2(p\text{-cymene})]_2$ and TsDPEN in water, the initial solution is acidic (pH ≈3), we also investigated the effect of acid on **1** in a similar manner. After abstracting the chloride from the ruthenium center with $NaBAr^F_4$ [BAr^F_4 = $B[3,5\text{-}C_6H_3(CF_3)_2)_4$], consecutive addition of DPPE and acid to the resulting solution generated an intermediate similar to **15** with a hemilabile DPPE, which is assigned on the similarity in their $^{31}P\{^1H\}$ NMR spectra (Figure S9). However, a DPPE-bridged ruthenium dimer **17** was recrystallized from the reaction solution, which has been characterized by X-ray crystallography (Figure 8). The protonation and subsequent loss of TsDPEN from the ruthenium center in the presence of an acid is in line with the loss of both catalyst activity and enantioselectivity when running the ATH under acidic conditions. The ease of this reaction is alarming particularly for commercial applications.

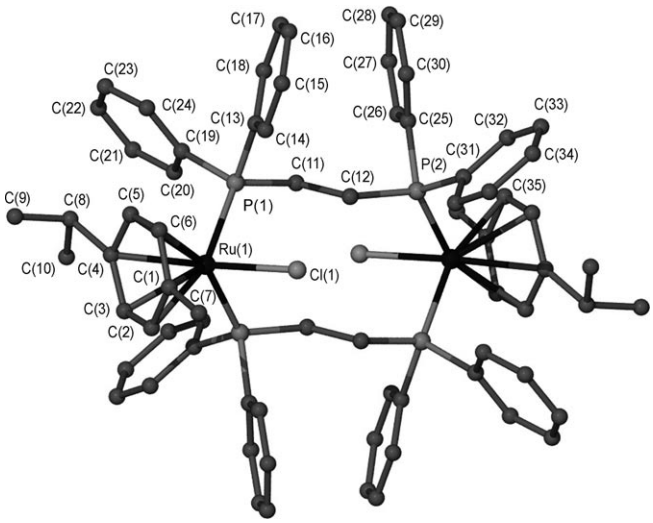

Figure 8. X-ray structure of **17** in $[\mathbf{17}][BArF_4]_2$ ($Ar^F = 3,5\text{-}C_6H_3(CF_3)_2$). The hydrogen atoms and anions are omitted for clarity. Selected distances [Å] and bond angles [°]: Ru(1)–P(1) 2.3751(8), Ru(1)–P(2) 2.3706(7), Ru(1)–Cl(1) 2.4052(8), P(1)-Ru(1)-P(2) 98.65(3), P(1)-Ru(1)-Cl(1) 88.57(3), P(2)-Ru(1)-Cl(1) 85.60(2).

It is noted that the coordination/dissociation of DPPE and TsDPEN is pH-dependent and reversible. Thus, in the presence of 1 equiv DPPE, the loss in the ATH reaction rate at low solution pH can be gradually recovered by adjusting the solution pH back to neutral or slightly basic.[5c,12d]

In contrast, having a higher affinity for Ru^{II}, bipy irreversibly displaces TsDPEN from the ruthenium center under acidic conditions, poisoning the catalysis "permanently".[5c,12d] Consistent with this observation, addition of bipy to a CH_2Cl_2 solution of **1**, acidified with slightly excess HPF_6, afforded the mononuclear ruthenium compound [RuCl(bipy)(*p*-cymene)][PF_6] as the only product isolated, which has been characterized by X-ray crystallography (see section 14, Supporting Information).

Discussion

Kinetics and mechanism: The results presented above suggest that ATH of acp in an aqueous solution follows a mechanistic pathway similar to ATH in organic solvents but with significant difference. In both cases, the reduction proceeds via the formato intermediate **2**, hydride **3** and the coordinatively unsaturated **4** (Scheme 4). However, in contrast with ATH in isopropanol where the rates are limited by the step of hydride formation,[3e] the aqueous ATH with formate features a fast step of hydride formation, with the ATH rate being controlled by hydrogen transfer from **3** to the carbonyl substrate. This is made manifest by the overall second-order kinetics over the concentration of catalyst and substrate in the ATH of acp in DMF/H_2O. The rate law suggests that the ATH is rate-limited by the hydrogen transfer step, with a transition state involving the catalyst and acp. The insignificant effect of the concentration of formate under the reaction conditions shows that the formation of the hydride **3** is unlikely to be rate-determining. This is further supported by the coexistence of the resonances of $HCOO^-$, Ru-H (**3**), and acp in the ^1H NMR study of a working catalytic solution.

The apparent activation parameters of the overall ATH of acp in DMF/H_2O are $\Delta H^{\neq} = 12.8\ kcal\,mol^{-1}$ and $\Delta S^{\neq} = -25.0\ cal\,K^{-1}\,mol^{-1}$, which are indicative of an organized transition state. However, the kinetics cannot be used to judge if the transition state is concerted, that is, **TS-A** in Scheme 6. Insight into this issue is gained through the KIE measurements and more importantly, DFT calculations; the latter show that, unlike the hydrogen transfer in organic media, the analogous process in water is step-wise.

Acceleration of ATH by water: Many examples of water-accelerated organic reactions have been reported,[6a,b,20d–f,42] and the excellent performance of Ru–TsDPEN in aqueous ATH are now well documented.[1n,5,7,8] However, the role of water in the ATH reactions has not been clearly defined.[1n] When the ATH of acp is performed in neat water, the reaction is biphasic and is diffusion limited. Surprisingly, this biphasic feature does not prevent an efficient ATH reaction (Figure S2). The accelerating effect of water on the reaction rate is readily seen in the stoichiometric reaction of the ruthenium hydride **3** and acp: the reduction rate was increased six-fold by just adding about 0.2% water. This cannot be attributed to a solvent effect and is a clear indication that water molecules participate in the transition state of the rate-limiting hydrogen transfer step.

The participation of water in the transition state is borne out by the DFT calculations, which show that water acts as a hydrogen bond donor, interacting with the ketone oxygen lone pair during hydrogen transfer (**TS-B**, Scheme 8 and 10). Significantly, this interaction lowers the reaction barrier of hydrogen transfer to acp by about 4 $kcal\,mol^{-1}$ with respect to the gas-phase transition state **TS-A**. Previous studies have disclosed hydrogen bonding as a key factor responsible for the rate acceleration of organic reactions in aqueous solution,[43] and in the case of Diels–Alder reactions, a similar lowering in the energy barrier by water has been calculated/measured recently.[6b,20f,41a,d,e,43]

Furthermore, water may also participate in the decarboxylation step. The activation barrier for the decarboxylation of **2** to give **3** could be reduced when the reaction is carried out in water. Water is known to accelerate CO_2 hydrogenation to form formic acid with ruthenium catalysts; this has been extensively studied both experimentally and theoretically.[44] Following the principle of microscopic reversibility, water should also promote its reverse reaction, decarboxylation of metal formate. Still further, water may facilitate the formation of **1**, presumably by hydrogen bonding with the chloride.[40] This is substantiated by the easy, quantitative synthesis of **1** from [$RuCl_2(\eta^6$-cymene)]$_2$ and TsDPEN in neat water.

Stabilization of active catalyst with water: The lifetime of the ruthenium catalyst in ATH reactions is remarkably elongated by water. This is clearly demonstrated by the experiments shown in Figure S10 (Supporting Information). In the presence of water, the Ru–TsDPEN catalyst was stable for up to a few months, as indicated by the little color change, and by the catalyst activity in an ATH reaction, in which only a slightly decreased rate was observed after the catalyst had been left in water for two months and then re-tested. In contrast, the catalyst life time was significantly shortened when water was removed from the solution, and in diethyl ether, the catalyst was very unstable, being totally decomposed in half an hour. In a previous study of a PEG-supported Ru–TsDPEN catalyst, we showed that the catalyst could be reused 14 times without affecting the *ee* values when the ATH was run in water; in its absence the recycle could not be repeated more than two times.[5b] Clearly, water stabilizes some key catalytic species. Whilst the details remain to be delineated, the reaction of water with **4** is illuminating. This has been studied by variable temperature ^1H NMR measurements, which suggests that water reacts with the reactive Ru–NH center, turning it into Ru-OH and -NH_2 (Scheme 11). The hydroxyl group undergoes exchange with bulk water even at low temperature, as demonstrated by ^1H NMR with alternative addition of H_2O/D_2O; but it does not appear to block the reaction with formate to generate **2** under neutral conditions. Thus, water may stabilize the 16-electron **4** by converting it into the hydroxyl species **14**, particularly when the concentration of substrate is low.[9]

However, the stability of the hydride **3** in the presence of water is less clear. Rauchfuss and co-workers have recently shown that the iridium analogue of **3** readily reacts with O_2, forming an analogue of **4**.[25] We also note that Ru–TsDPEN is less stable than the analogous iridium catalyst in aqueous-phase ATH in open air.[5i] Indeed, very recent work from Ikariya and co-workers suggests that **3** may also react with O_2.[45]

Under more basic conditions, the hydroxide would compete with formate for coordination to Ru^{II}. This partly explains why ATH becomes slower at high pH; high pH will also slow down the reaction at a constant $[CO_2]$ according to the rate law in Scheme 5.[5i,32] Indeed, similar iridium hydroxyl complexes have been shown to be inactive for ATH under basic conditions.[10a,c,39,46] Recently, *trans*-[RuH(OH)((*R*)-BINAP)((*R*,*R*)-DPEN)] was isolated in the presence of KO*t*Bu and trace water, showing no reaction with hydrogen.[47]

Conclusion

This study represents the first, systematic investigation of the reaction mechanism of ATH reactions in water. By using stoichiometric reactions, NMR probing, kinetic and isotope effect measurements, DFT modeling, and X-ray structure analysis, we are able to establish:

1) Ruthenium–hydride **3** and the 16-electron species **4**, which are involved in the catalytic cycle of ATH in organic media, are active catalysts in ATH in water. The chloride **1** is a precatalyst, which is instantly converted into **3** upon the introduction of formate; the formato complex **2** could not be detected in either stoichiometric or catalytic reactions. Under these conditions, however, **3** is visible in the NMR spectra. On the other hand, the decarboxylation of **2** to give **3** is reversible. The kinetic profiles of ATH of acp with **1**, **3** and **4** show no significant difference; thus the complexes **2**–**4** of Scheme 4 are all involved in the aqueous-phase ATH.
2) Water accelerates the ATH reaction, and the ruthenium catalyst is much more stable in the presence of water. In stoichiometric reduction of acp by the hydride **3**, the rate in wet CD_2Cl_2 is six times that in dry CD_2Cl_2. In catalytic ATH of acp in DMF, the addition of water can easily accelerate the reaction by more than 50-fold.
3) Both **1** and **3** are protonated at the amido nitrogen of their TsDPEN ligand under acidic conditions, leading to ring-opening of the chelating ligand. In the case of **3**, protonation may also occur at the hydride. Under neutral conditions, water coordinates to **4**, presumably forming the aqua species **13** and hydroxyl species **14**.
4) The rate of ATH of acp is first order in both the catalyst and ketone substrate, and is inhibited by CO_2. Under normal ATH conditions in aqueous formate, however, the concentration of free CO_2 is low. Both the kinetic and NMR measurements agree with the hydrogen transfer from ruthenium to ketone being the rate-limiting step, and this is associated with a large negative activation entropy of $-25.0\,cal\,K^{-1}\,mol^{-1}$. These studies point to a transition state resembling that proposed by Noyori and Ikariya for non-aqueous media, namely, **TS-A** in Scheme 6.
5) DFT calculations show that water participates in the transition state of hydrogen transfer, giving rise to **TS-B**, which is stabilized by water by about $4\,kcal\,mol^{-1}$ through hydrogen bonding, with water acting as hydrogen bond donor. The calculations also reveal that the hydrogen transfer step is more step-wise rather than concerted.
6) Significant kinetic isotope effects are measured for k_{RuHNH}/k_{RuHND}, k_{RuHNH}/k_{RuDNH}, and k_{RuHNH}/k_{RuDND}, which is in line with ATH being controlled by the hydrogen transfer. However, the product of the first two values deviates significantly from the last one, possibly due to H–D scrambling and the step-wise nature of the hydrogen transfer step.

On the basis of the results presented and Scheme 4, we proposed a revised mechanism for the ATH reactions in water. As is illustrated in Scheme 13, the aqueous-phase reduction may proceed along three different directions depending on the solution pH. The cycle under neutral conditions is most efficient, affording fast rates and high enantioselectivity via a water-assisted transition state. Under acidic conditions, protonation occurs at both the hydride and the TsDPEN ligand, leading to lower catalytic activity and lower *ee* values. However, higher pH drives the catalyst into the hydroxyl form, thus decreasing the concentration of active catalyst and so the reduction rates, albeit without affecting the *ee* values.

The role of water is worth further highlighting. It appears to be involved in the whole catalytic cycle. Firstly, it acts as a base to assist the dehydrochlorination of catalyst precursor to generate the precatalyst **1**. Secondly, it presumably facilitates the decarboxylation of the formato intermediate **2** to form the hydride **3**. Thirdly, water interacts with the 16-electron complex **4**, stabilizing it as an aqua/hydroxyl species. And finally, it participates in the transition state of hydrogen transfer by hydrogen bonding to the ketone oxygen atom. Not only does this hydrogen bonding lower the transition barrier, it also changes the mode of hydrogen transfer from being concerted to step-wise.

Experimental Section

General: All manipulations were conducted under nitrogen or argon atmosphere using standard Schlenk techniques. All solvents except water were purchased from Aldrich and freshly distilled under inert atmosphere before use. Deuterated solvents were degassed by freezing, evacuating, and thawing (3×), and were then dried over 4 Å sieves and stored under nitrogen. ^1H, $^{13}C\{^1H\}$, $^{31}P\{^1H\}$ and ^2H NMR spectra were obtained using a Bruker Avance 400 MHz spectrometer. Chemical shifts are reported in parts per million (δ) relative to residual protic solvent, and cou-

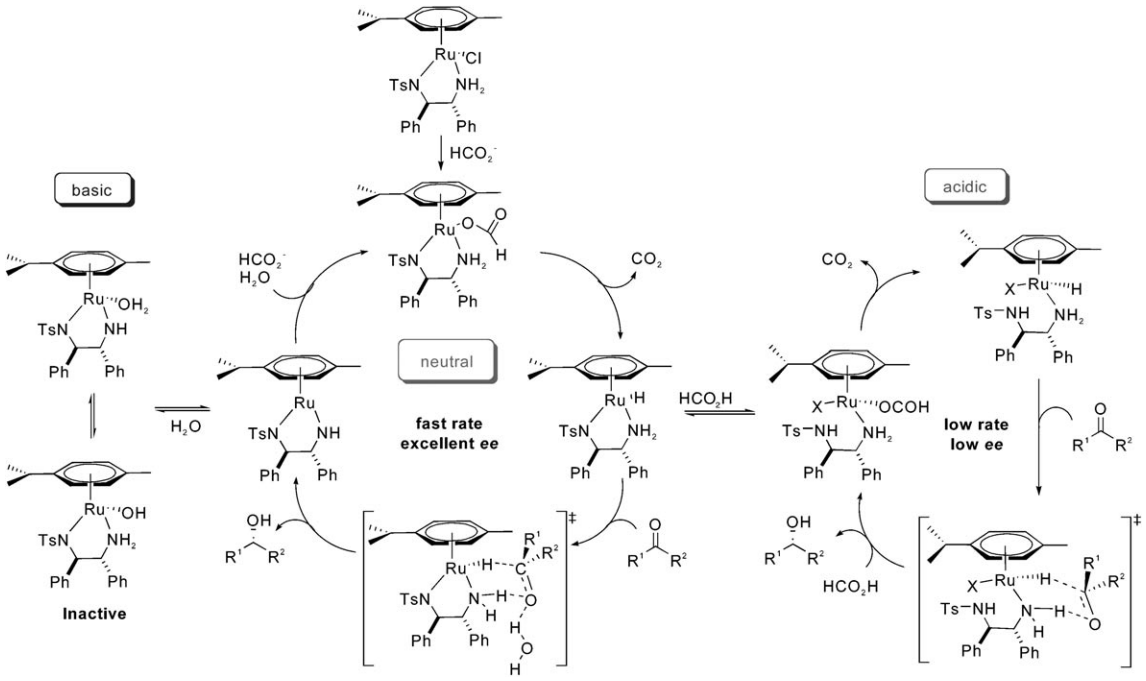

Scheme 13. Proposed mechanism for ATH in water at different pH (In the acidic cycle, X may be the formate anion; if X is water, each species should be +1 charged; water may also participate in the TS).

pling constants are reported in Hertz (Hz). Unless otherwise noted, samples for NMR analysis were prepared in CD_2Cl_2. Sodium tetrakis[3,5-bis(trifluoromethyl)phenyl] borate was purchased from Aldrich. [RuCl(TsDPEN)(*p*-cymene)] (**1**), [RuH(TsDPEN)(*p*-cymene)] (**3**), and [Ru(TsDPEN-H)(*p*-cymene)] (**4**) were synthesized according to literature procedures.[3e] Described below are selected experiments that are discussed in detail in the text; further experimental details are found in the Supporting Information.

Synthesis of 1 in water: $[RuCl_2(p\text{-cymene})]_2$ (31 mg, 0.5 mmol) and TsDPEN (44 mg, 1.2 mmol) were placed in a Schlenk tube equipped with a magnetic stirrer bar under nitrogen. Water (10 mL, distilled, degassed) was added to the flask and the suspension was heated to 40 °C. A pale yellow orange precipitate was formed after stirring at 40 °C for 1 h, which was then extracted with CH_2Cl_2 (2×3 mL), washed with water (2×3 mL) and dried under vacuum. The compound, obtained in almost quantitative yield, was identified as **1** by its identical X-ray crystal structure and NMR spectra to the same compound synthesized as described in the literature.[3e]

Reaction of 3 in the presence of DPPE: Ruthenium hydride **3** (69 mg, 0.12 mmol) and 1 equiv DPPE (46 mg) was placed in a Schlenk tube equipped with a teflon-coated magnetic stirrer bar; CD_2Cl_2 (1 mL) was added. To the above solution, CF_3SO_3H (ca. 2 equiv) was then added successively in small portions and the reaction was monitored by $^{31}P\{^1H\}$ NMR at −30 °C. **15** and **16** were detected as the major products. Pale yellow crystals of $[Ru(\eta^1\text{-TsDPEN})(\eta^6\text{-cymene})(\eta^2\text{-DPPE})][CF_3SO_3]_2$ (**16-$[CF_3SO_3]_2$**) were obtained from a dichloromethane solution at −30 °C.

Stoichiometric ATH of acp: The ruthenium hydride **3** (5 mg, 8 μmmol) was dissolved in CD_2Cl_2 (0.5 mL) containing ferrocene (1 mg) as internal standard. After cooling to −80 °C, 1 equiv acp was syringed into in the NMR tube and the tube was carefully shaken. The sample was then put into the spectrometer and quickly locked and shimmed. The reaction was then followed by ^1H NMR at 20 °C by integrating the peaks of ferrocene, acp, and 1-phenylethanol. The same reaction was carried out in CD_2Cl_2 doped with 0.2 % H_2O.

ATH of acp: The ATH reaction was normally carried out under the optimized reaction, i.e., in a mixture of DMF/H_2O 1:1 (distilled, degassed) at 40 °C with a stirring speed of 1200 rpm, with the precatalyst generated in situ. After incubating a mixture of 0.005 mmol $[RuCl_2(p\text{-cymene})]_2$ and 1.2 equiv TsDPEN in DMF/H_2O (2 mL) at 40 °C for 1 hour, the reaction was initiated by adding HCOONa and then acp. The reaction solution was sampled at desired time and analyzed by a Varian CP-3380 GC equipped with a Chrompack Chirasil-Dex CB column (25 m × 0.25 mm). Kinetic isotope effects were examined in a similar manner except that deuterated reagent/solvent was used. When necessary, the product was isolated by flash chromatography (silica gel, hexane/ethyl acetate 8:1).

Computational details: Geometries of the transition states, intermediates and separated reactants were optimized using the DMol^3 code from Accelerys (Material Studio 3.2),[48] using the BLYP density functional.[49] In DMol^3 the electronic wave function is expanded in a localized atom-centered basis set with each basis function defined numerically on a dense radial grid. The inner core electrons for Ru were represented by the DFT semi-local pseudo-potential specifically developed for DMol^3 calculations, while sixteen electrons were treated explicitly for Ru (those corresponding to the atomic levels 4s, 4p, 4d, 5s). We used the double-numeric-polarized (DNP) basis sets, which are variationally comparable to the 6-31G(d,p) basis sets. However, the numerical functions are far more complete than the traditional Gaussian functions. Each basis function was restricted to within a cutoff radius of $R_{cut}=4.7$ Å. This basis set is referred to as BS-I. The electron density was approximated using a multipolar expansion up to octupole. We have chosen the BLYP/BS-I level of theory to obtain the geometries of the transition states, intermediates and separated reactants on the basis of a previous computational study of Ru(diamine)-catalysed ketone hydrogenation.[50]

The Gamess UK program[51] was employed to obtain more accurate energetics from single-point energy calculations using the BB1K functional,[52] which was specifically developed for accurate calculation of kinetics. For ruthenium, we considered the LANL2 effective core potential to describe the inner core electrons together with the [1f,3d,4p,s] valence basis (obtained by uncontracting the outer basis function primitives of the LANL2DZ basis set to triple-zeta using the "even-tempered" method to obtain the exponents, and augmented with one f-polarization function, $\zeta=1.235$[53]). The 6-311++G(2df,2pd) was used for H, C, N, O. This basis set is referred to as BS-II.

The minimum and saddle point character of all optimized structures were verified by evaluation of the harmonic vibrational frequencies.

X-ray structure determination: A suitable crystal of **[16]-$[CF_3SO_3]_2$·CH_2Cl_2** was chosen and mounted on a glass fiber. X-ray crystallographic data were collected on a Bruker D8 Diffractometer at 100 K (−173 °C) using $Mo_{K\alpha}$ graphite monochromated radiation (λ = 0.71073 Å). The structure was solved by direct methods using the program SHELXS-97 and refined by full matrix least squares on F^2 with SHELXL-97. The structures of **17** and [RuCl(bipy)(η^6-cymene)][PF_6] were determined in a similar manner. See the Supporting Information for details.

CCDC 677270 (**16**), 677272 (**17**), and 677271 ([RuCl(bipy)(η^6-cymene)]-[PF_6]) contain the supplementary crystallographic data for this paper. These data can be obtained free of charge from the Cambridge Crystallographic Data Centre via www.ccdc.cam.ac.uk/data_request/cif.

Acknowledgements

We gratefully acknowledge the DTI Manufacturing Molecules Initiatives (MMI) and EPSRC (EP/C005643/1) for studentship and postdoctoral fellowships (X.W., J.L., D.D.T.), and the industrial and academic partners of the MMI project for financial support and invaluable suggestions: Drs. F. Hancock, A. Zanotti-Gerosa and S. A. French, Johnson Matthey; Dr. A. Pettman, Pfizer; Drs. P. Hogan and M. Purdie, AstraZeneca; Dr. P. Ravenscroft, GlaxoSmithKline; Dr. A. Danopoulos, University of Southampton. We also thank Professor Don Bethell for helpful discussions.

[1] Reviews on ATH: a) R. Noyori, S. Hashiguchi, *Acc. Chem. Res.* **1997**, *30*, 97; b) M. J. Palmer, M. Wills, *Tetrahedron: Asymmetry* **1999**, *10*, 2045; c) M. Wills, M. Palmer, A. Smith, J. Kenny, T. Walsgrove, *Molecules* **2000**, *5*, 4; d) C. Saluzzo, M. Lemaire, *Adv. Synth. Catal.* **2002**, *344*, 915; e) H. U. Blaser, C. Malan, B. Pugin, F. Spindler, H. Steiner, M. Studer, *Adv. Synth. Catal.* **2003**, *345*, 103; f) K. Everaere, A. Mortreux, J. F. Carpentier, *Adv. Synth. Catal.* **2003**, *345*, 67; g) J. Blacker, J. Martin, in *Asymmetric Catalysis on Industrial Scale: Challenges, Approaches and Solutions* (Eds.: H. U. Blaser, E. Schmidt), Wiley, **2004**, pp. 210–216; h) S. E. Clapham, A. Hadzovic, R. H. Morris, *Coord. Chem. Rev.* **2004**, *248*, 2201; i) E. Peris, R. H. Crabtree, *Coord. Chem. Rev.* **2004**, *248*, 2239; j) S. Gladiali, E. Alberico, *Chem. Soc. Rev.* **2006**, *35*, 226; k) T. Ikariya, K. Murata, R. Noyori, *Org. Biomol. Chem.* **2006**, *4*, 393; l) D. Mery, D. Astruc, *Coord. Chem. Rev.* **2006**, *250*, 1965; m) J. S. M. Samec, J. E. Bäckvall, P. G. Andersson, P. Brandt, *Chem. Soc. Rev.* **2006**, *35*, 237; n) X. F. Wu, J. L. Xiao, *Chem. Commun.* **2007**, 2449; o) P. Roszkowski, Z. Czarnocki, *Mini-Rev. Org. Chem.* **2007**, *4*, 190; p) S. L. You, *Chem. Asian J.* **2007**, *2*, 820.

[2] In this article, Ru-TsDPEN refers to, without specifying X [Eq. (1)], catalysts derived from [$RuCl_2$(*p*-cymene)]$_2$ and TsDPEN with the hydrogen on the sulfonylated nitrogen being removed.

[3] a) S. Hashiguchi, A. Fujii, J. Takehara, T. Ikariya, R. Noyori, *J. Am. Chem. Soc.* **1995**, *117*, 7562; b) A. Fujii, S. Hashiguchi, N. Uematsu, T. Ikariya, R. Noyori, *J. Am. Chem. Soc.* **1996**, *118*, 2521; c) J. Takehara, S. Hashiguchi, A. Fujii, S. Inoue, T. Ikariya, R. Noyori, *Chem. Commun.* **1996**, 233; d) N. Uematsu, A. Fujii, S. Hashiguchi, T. Ikariya, R. Noyori, *J. Am. Chem. Soc.* **1996**, *118*, 4916; e) K. J. Haack, S. Hashiguchi, A. Fujii, T. Ikariya, R. Noyori, *Angew. Chem.* **1997**, *109*, 297; *Angew. Chem. Int. Ed. Engl.* **1997**, *36*, 285; f) S. Hashiguchi, A. Fujii, K. J. Haack, K. Matsumura, T. Ikariya, R. Noyori, *Angew. Chem.* **1997**, *109*, 300; *Angew. Chem. Int. Ed. Engl.* **1997**, *36*, 288.

[4] Selected recent examples of ATH: a) D. W. Wang, W. Zeng, Y. G. Zhou, *Tetrahedron: Asymmetry* **2007**, *18*, 1103; b) T. S. Venkatakrishnan, S. K. Mandal, R. Kannan, S. S. Krishnamurthy, M. Nethaji, *J. Organomet. Chem.* **2007**, *692*, 1875; c) W. Y. Shen, H. Zhang, H. L. Zhang, J. X. Gao, *Tetrahedron: Asymmetry* **2007**, *18*, 729; d) T. Privalov, J. S. M. Samec, J. E. Bäckvall, *Organometallics* **2007**, *26*, 2840; e) Y. Nishibayashi, Y. Miyake, S. Uemura, *J. Synth. Org. Chem. Jpn.* **2007**, *65*, 761; f) G. B. Ma, R. McDonald, M. Ferguson, R. G. Cavell, B. O. Patrick, B. R. James, T. Q. Hu, *Organometallics* **2007**, *26*, 846; g) X. H. Huang, J. Y. Ying, *Chem. Commun.* **2007**, 1825; h) S. Enthaler, B. Hagemann, S. Bhor, G. Anilkumar, M. K. Tse, B. Bitterlich, K. Junge, G. Erre, M. Beller, *Adv. Synth. Catal.* **2007**, *349*, 853; i) J. Ekstrom, J. Wettergren, H. Adolfsson, *Adv. Synth. Catal.* **2007**, *349*, 1609; j) F. K. Cheung, A. M. Hayes, D. J. Morris, M. Wills, *Org. Biomol. Chem.* **2007**, *5*, 1093; k) M. C. Carrion, F. A. Jalon, B. R. Manzano, A. M. Rodriguez, F. Sepulveda, M. Maestro, *Eur. J. Inorg. Chem.* **2007**, 3961; l) A. B. Zaitsev, H. Adolfsson, *Org. Lett.* **2006**, *8*, 5129; m) R. V. Wisman, J. G. de Vries, B. J. Deelman, H. J. Heeres, *Org. Process Res. Dev.* **2006**, *10*, 423; n) P. Vastila, A. B. Zaitsev, J. Wettergren, T. Privalov, H. Adolfsson, *Chem. Eur. J.* **2006**, *12*, 3218; o) C. V. Ursini, F. Mazzeo, J. A. R. Rodrigues, *Tetrahedron: Asymmetry* **2006**, *17*, 3335; p) M. T. Reetz, X. G. Li, *J. Am. Chem. Soc.* **2006**, *128*, 1044; q) D. J. Morris, A. M. Hayes, M. Wills, *J. Org. Chem.* **2006**, *71*, 7035; r) K. Mikami, K. Wakabayashi, Y. Yusa, K. Aikawa, *Chem. Commun.* **2006**, 2365; s) C. Letondor, A. Pordea, N. Humbert, A. Ivanova, S. Mazurek, M. Novic, T. R. Ward, *J. Am. Chem. Soc.* **2006**, *128*, 8320; t) S. Fukuzawa, T. Suzuki, *Eur. J. Org. Chem.* **2006**, 1012; u) J. B. Sortais, V. Ritleng, A. Voelklin, A. Holuigue, H. Smail, L. Barloy, C. Sirlin, G. K. M. Verzijl, J. A. F. Boogers, A. H. M. de Vries, J. G. de Vries, M. Pfeffer, *Org. Lett.* **2005**, *7*, 1247; v) R. W. Guo, C. Elpelt, X. H. Chen, D. T. Song, R. H. Morris, *Chem. Commun.* **2005**, 3050; w) K. Fujita, R. Yamaguchi, *Synlett* **2005**, 560; x) F. K. Cheung, A. M. Hayes, J. Hannedouche, A. S. Y. Yim, M. Wills, *J. Org. Chem.* **2005**, *70*, 3188; y) K. Aboulaala, C. Goux-Henry, D. Sinou, M. Safi, M. Soufiaoui, *J. Mol. Catal. A* **2005**, *237*, 259; z) G. Venkatachalam, R. Ramesh, *Inorg. Chem. Commun.* **2005**, *8*, 1009.

[5] a) X. F. Wu, X. G. Li, W. Hems, F. King, J. L. Xiao, *Org. Biomol. Chem.* **2004**, *2*, 1818; b) X. G. Li, X. F. Wu, W. P. Chen, F. Hancock, F. King, J. L. Xiao, *Org. Lett.* **2004**, *6*, 3321; c) X. F. Wu, X. G. Li, F. King, J. L. Xiao, *Angew. Chem.* **2005**, *117*, 3473; *Angew. Chem. Int. Ed.* **2005**, *44*, 3407; d) X. F. Wu, D. Vinci, T. Ikariya, J. L. Xiao, *Chem. Commun.* **2005**, 4447; e) J. L. Xiao, X. F. Wu, A. Zanotti-Gerosa, F. Hancock, *Chim. Oggi-Chem. Today* **2005**, *23*, 50; f) X. F. Wu, X. H. Li, M. McConville, O. Saidi, J. L. Xiao, *J. Mol. Catal. A* **2006**, *247*, 153; g) X. H. Li, J. Blacker, I. Houson, X. F. Wu, J. L. Xiao, *Synlett* **2006**, 1155; h) X. F. Wu, J. K. Liu, X. H. Li, A. Zanotti-Gerosa, F. Hancock, D. Vinci, J. W. Ruan, J. L. Xiao, *Angew. Chem.* **2006**, *118*, 6870; *Angew. Chem. Int. Ed.* **2006**, *45*, 6718; i) X. F. Wu, X. H. Li, A. Zanotti-Gerosa, A. Pettman, J. K. Liu, A. J. Mills, J. L. Xiao, *Chem. Eur. J.* **2008**, *14*, 2209; j) X. F. Wu, C. Corcoran, S. J. Yang, J. L. Xiao, *ChemSusChem* **2008**, *1*, 71.

[6] Recent reviews on catalysis in water: a) C. J. Li, L. Chen, *Chem. Soc. Rev.* **2006**, *35*, 68; b) M. C. Pirrung, *Chem. Eur. J.* **2006**, *12*, 1312; c) U. M. Lindstrom, F. Andersson, *Angew. Chem.* **2006**, *118*, 562; *Angew. Chem. Int. Ed.* **2006**, *45*, 548; d) *Aqueous-Phase Organometallic Catalysis: Concepts and Applications*; B. Cornils, W. A. Herrmann, Eds.; Wiley-VCH: Weinheim, **2004**; e) S. Kobayashi, K. Manabe, *Acc. Chem. Res.* **2002**, *35*, 209; f) F. Joo, *Acc. Chem. Res.* **2002**, *35*, 738.

[7] Recent examples of ATH in water: a) P. N. Liu, J. G. Deng, Y. Q. Tu, S. H. Wang, *Chem. Commun.* **2004**, 2070; b) K. Micskei, C. Hajdu, L. A. Wessjohann, L. Mercs, A. Kiss-Szikszai, T. Patonay, *Tetrahedron: Asymmetry* **2004**, *15*, 1735; c) V. Miranda-Soto, M. Parra-Hake, D. Morales-Morales, R. A. Toscano, G. Boldt, A. Koch, D. B. Grotjahn, *Organometallics* **2005**, *24*, 5569; d) P. N. Liu, P. M. Gu, J. G. Deng, Y. Q. Tu, Y. P. Ma, *Eur. J. Org. Chem.* **2005**, 3221; e) C. Letondor, N. Humbert, T. R. Ward, *Proc. Natl. Acad. Sci. USA* **2005**, *102*, 4683; f) J. C. Mao, B. S. Wan, F. Wu, S. W. Lu, *Tetrahedron Lett.* **2005**, *46*, 7341; g) F. Wang, H. Liu, L. F. Cun, J. Zhu, J. G. Deng, Y. Z. Jiang, *J. Org. Chem.* **2005**, *70*, 9424; h) J. Canivet, G. Labat, H. Stoeckli-Evans, G. Süss-Fink, *Eur. J. Inorg. Chem.* **2005**, 4493; i) J. S. Wu, F. Wang, Y. P. Ma, X. C. Cui, L. F. Cun, J. Zhu, J. G. Deng, B. L. Yu, *Chem. Commun.* **2006**, 1766; j) Y. Arakawa, N. Haraguchi, S. Itsuno, *Tetrahedron Lett.* **2006**, *47*, 3239; k) Y. Xing,

J. S. Chen, Z. R. Dong, Y. Y. Li, J. X. Gao, *Tetrahedron Lett.* **2006**, *47*, 4501; l) L. Jiang, T. F. Wu, Y. C. Chen, J. Zhu, J. G. Deng, *Org. Biomol. Chem.* **2006**, *4*, 3319; m) S. Zeror, J. Collin, J. C. Fiaud, L. A. Zouioueche, *J. Mol. Catal. A* **2006**, *256*, 85; n) B. Z. Li, J. S. Chen, Z. R. Dong, Y. Y. Li, Q. B. Li, J. X. Gao, *J. Mol. Catal. A* **2006**, *258*, 113; o) N. A. Cortez, R. Rodriguez-Apodaca, G. Aguirre, M. Parra-Hake, T. Cole, R. Somanathan, *Tetrahedron Lett.* **2006**, *47*, 8515; p) D. M. Jiang, J. S. Gao, Q. H. Yang, J. Yang, C. Li, *Chem. Mater.* **2006**, *18*, 6012; q) D. S. Matharu, D. J. Morris, G. J. Clarkson, M. Wills, *Chem. Commun.* **2006**, 3232; r) N. A. Cortez, G. Aguirre, M. Parra-Hake, R. Somanathan, *Tetrahedron Lett.* **2007**, *48*, 4335; s) L. Li, J. S. Wu, F. Wang, J. Liao, H. Zhang, C. X. Lian, J. Zhu, J. G. Deng, *Green Chem.* **2007**, *9*, 23; t) J. Canivet, G. Süss-Fink, *Green Chem.* **2007**, *9*, 391; u) H. F. Zhou, Q. H. Fan, Y. Y. Huang, L. Wu, Y. M. He, W. J. Tang, L. Q. Gu, A. S. C. Chan, *J. Mol. Catal. A* **2007**, *275*, 47; v) S. Itsuno, M. Takahashi, Y. Arakawa, N. Haraguchi, *Pure Appl. Chem.* **2007**, *79*, 1471.

[8] Earlier examples of ATH in water: a) C. Bubert, J. Blacker, S. M. Brown, J. Crosby, S. Fitzjohn, J. P. Muxworthy, T. Thorpe, J. M. J. Williams, *Tetrahedron Lett.* **2001**, *42*, 4037; b) T. Thorpe, J. Blacker, S. M. Brown, C. Bubert, J. Crosby, S. Fitzjohn, J. P. Muxworthy, J. M. J. Williams, *Tetrahedron Lett.* **2001**, *42*, 4041; c) H. Y. Rhyoo, H. J. Park, Y. K. Chung, *Chem. Commun.* **2001**, 2064; d) H. Y. Rhyoo, H. J. Park, W. H. Suh, Y. K. Chung, *Tetrahedron Lett.* **2002**, *43*, 269; e) Y. Himeda, N. Onozawa-Komatsuzaki, H. Sugihara, H. Arakawa, K. Kasuga, *J. Mol. Catal. A* **2003**, *195*, 95; f) Y. P. Ma, H. Liu, L. Chen, X. Cui, J. Zhu, J. G. Deng, *Org. Lett.* **2003**, *5*, 2103; g) A. N. Ajjou, J. L. Pinet, *J. Mol. Catal. A* **2004**, *214*, 203.

[9] T. Ikariya, A. J. Blacker, *Acc. Chem. Res.* **2007**, *40*, 1300.

[10] a) S. Ogo, T. Abura, Y. Watanabe, *Organometallics* **2002**, *21*, 2964; b) S. Ogo, N. Makihara, Y. Watanabe, *Organometallics* **1999**, *18*, 5470; c) S. Ogo, N. Makihara, Y. Kaneko, Y. Watanabe, *Organometallics* **2001**, *20*, 4903; d) T. Abura, S. Ogo, Y. Watanabe, S. Fukuzumi, *J. Am. Chem. Soc.* **2003**, *125*, 4149.

[11] Examples of pH-rate dependence in hydrogenation: a) F. Joo, J. Kovacs, A. C. Benyei, A. Katho, *Angew. Chem.* **1998**, *110*, 1024; *Angew. Chem. Int. Ed.* **1998**, *37*, 969; b) F. Joo, J. Kovacs, A. C. Benyei, A. Katho, *Catal. Today* **1998**, *42*, 441; c) F. Joo, J. Kovacs, A. C. Benyei, L. Nadasdi, G. Laurenczy, *Chem. Eur. J.* **2001**, *7*, 193; d) G. Laurenczy, F. Joo, L. Nadasdi, *Inorg. Chem.* **2000**, *39*, 5083; e) G. Papp, J. Elek, L. Nadasdi, G. Laurenczy, F. Joo, *Adv. Synth. Catal.* **2003**, *345*, 172; f) H. H. Horvath, F. Joo, *React. Kinet. Catal. Lett.* **2005**, *85*, 355; g) C. A. Mebi, B. J. Frost, *Organometallics* **2005**, *24*, 2339; Examples of pH-rate dependence in transfer hydrogenation: h) S. Ogo, K. Uehara, T. Abura, Y. Watanabe, S. Fukuzumi, *J. Am. Chem. Soc.* **2004**, *126*, 16520; i) S. Ogo, H. Nishida, H. Hayashi, Y. Murata, S. Fukuzumi, *Organometallics* **2005**, *24*, 4816; j) C. A. Mebi, R. P. Nair, B. J. Frost, *Organometallics* **2007**, *26*, 429.

[12] a) D. G. Blackmond, M. Ropic, M. Stefinovic, *Org. Process Res. Dev.* **2006**, *10*, 457; b) M. Miyagi, J. Takehara, S. Collet, K. Okano, *Org. Process Res. Dev.* **2000**, *4*, 346; c) K. Tanaka, M. Katsurada, F. Ohno, Y. Shiga, M. Oda, M. Miyagi, J. Takehara, K. Okano, *J. Org. Chem.* **2000**, *65*, 432; d) X. F. Wu, PhD thesis, University of Liverpool, **2007**.

[13] a) M. Yamakawa, H. Ito, R. Noyori, *J. Am. Chem. Soc.* **2000**, *122*, 1466; b) R. Noyori, M. Yamakawa, S. Hashiguchi, *J. Org. Chem.* **2001**, *66*, 7931.

[14] C. P. Casey, J. B. Johnson, *J. Org. Chem.* **2003**, *68*, 1998.

[15] a) J. B. Johnson, J. E. Bäckvall, *J. Org. Chem.* **2003**, *68*, 7681; b) C. P. Casey, J. B. Johnson, *Can. J. Biochem.* **2005**, *83*, 1339; c) C. P. Casey, S. W. Singer, D. R. Powell, R. K. Hayashi, M. Kavana, *J. Am. Chem. Soc.* **2001**, *123*, 1090.

[16] a) L. Y. Kuo, T. J. R. Weakley, K. Awana, C. Hsia, *Organometallics* **2001**, *20*, 4969; b) L. Y. Kuo, D. M. Finigan, N. N. Tadros, *Organometallics* **2003**, *22*, 2422; c) C. S. Yi, Z. J. He, I. A. Guzei, *Organometallics* **2001**, *20*, 3641.

[17] a) A. H. Ell, J. B. Johnson, J. E. Bäckvall, *Chem. Commun.* **2003**, 1652; b) C. P. Casey, G. A. Bikzhanova, Q. Cui, I. A. Guzei, *J. Am. Chem. Soc.* **2005**, *127*, 14062; c) J. S. M. Samec, A. H. Ell, J. B. Aberg, T. Privalov, L. Eriksson, J. E. Bäckvall, *J. Am. Chem. Soc.* **2006**, *128*, 14293.

[18] a) J. B. Aberg, J. S. M. Samec, J. E. Bäckvall, *Chem. Commun.* **2006**, 2771; b) M. P. Magee, J. R. Norton, *J. Am. Chem. Soc.* **2001**, *123*, 1778; c) R. M. Bullock, *Chem. Eur. J.* **2004**, *10*, 2366; d) T. Ohkuma, N. Utsumi, K. Tsutsumi, K. Murata, C. Sandoval, R. Noyori, *J. Am. Chem. Soc.* **2006**, *128*, 8724.

[19] J. W. Handgraaf, E. J. Meijer, *J. Am. Chem. Soc.* **2007**, *129*, 3099.

[20] a) A. Ponti, G. Molteni, *New J. Chem.* **2002**, *26*, 1346; b) A. Rossin, G. Kovacs, G. Ujaque, A. Lledos, F. Joo, *Organometallics* **2006**, *25*, 5010; c) J. T. Henrikson, P. E. Savage, *Ind. Eng. Chem. Res.* **2004**, *43*, 4841; d) S. Narayan, J. Muldoon, M. G. Finn, V. V. Fokin, H. C. Kolb, K. B. Sharpless, *Angew. Chem.* **2005**, *117*, 3339; *Angew. Chem. Int. Ed.* **2005**, *44*, 3275; e) H. C. Hailes, *Org. Process Res. Dev.* **2007**, *11*, 114; f) Y. S. Jung, R. A. Marcus, *J. Am. Chem. Soc.* **2007**, *129*, 5492; g) G. Kovacs, G. Ujaque, A. Lledos, F. Joo, *Eur. J. Inorg. Chem.* **2007**, 2879; h) N. Zotova, A. Franzke, A. Amstrong, D. G. Blackmond, *J. Am. Chem. Soc.* **2007**, *129*, 15100.

[21] a) J. Canivet, L. Karmazin-Brelot, G. Süss-Fink, *J. Organomet. Chem.* **2005**, *690*, 3202; b) J. Canivet, B. Therrien, G. Süss-Fink, *Acta Crystallogr. Sect. E: Struct. Rep. Online* **2006**, *62*, M2435; c) P. Stepnicka, J. Ludvik, J. Canivet, G. Süss-Fink, *Inorg. Chim. Acta* **2006**, *359*, 2369.

[22] a) F. Wang, H. M. Chen, S. Parsons, L. D. H. Oswald, J. E. Davidson, P. J. Sadler, *Chem. Eur. J.* **2003**, *9*, 5810; b) A. F. A. Peacock, M. Melchart, R. J. Deeth, A. Habtemariam, S. Parsons, P. J. Sadler, *Chem. Eur. J.* **2007**, *13*, 2601.

[23] S. Ogo, R. Kabe, H. Hayashi, R. Harada, S. Fukuzumi, *Dalton Trans.* **2006**, 4657.

[24] a) J. Diez, M. P. Gamasa, E. Lastra, A. Garcia-Fernandez, M. P. Tarazona, *Eur. J. Inorg. Chem.* **2006**, 2855; b) D. J. Darensbourg, N. W. Stafford, F. Joo, J. H. Reibenspies, *J. Organomet. Chem.* **1995**, *488*, 99; c) T. Poth, H. Paulus, H. Elias, C. Ducker-Benfer, R. van Eldik, *Eur. J. Inorg. Chem.* **2001**, 1361.

[25] The related Ir^{III}–H complex is recently shown to be reactive towards O_2: a) Z. M. Heiden, T. B. Rauchfuss, *J. Am. Chem. Soc.* **2007**, *129*, 14303; b) Z. M. Heiden, T. B. Rauchfuss, *J. Am. Chem. Soc.* **2006**, *128*, 13048.

[26] T. Koike, T. Ikariya, *Adv. Synth. Catal.* **2004**, *346*, 37.

[27] a) K. Murata, H. Konishi, M. Ito, T. Ikariya, *Organometallics* **2002**, *21*, 253; b) D. Heller, A. H. M. de Vries, J. G. de Vries, in *Handbook of Homogeneous Hydrogenation* (Eds.: J. G. de Vries, C. J. Elsevier), Wiley-VCH, Weinheim, **2007**.

[28] C. Sandoval, T. Ohkuma, N. Utsumi, K. Tsutsumi, K. Murata, R. Noyori, *Chem. Asian J.* **2006**, *1*, 102.

[29] The reversibility of decarboxylation of the ruthenium formato intermediate is also supported by the observation that deuteration of HCOONa is catalyzed by the identical catalyst system with D_2O or $[D_4]$methanol as deuterium source (see Supporting Information).

[30] F. R. Keene, in *Electrochemical and Electrocatalytic Reactions of Carbon Dioxide* (Eds.: B. P. Sullivan, K. Krist, H. E. Guard), Elsevier, Amsterdam **1993**.

[31] A more appropriate treatment may make use of the steady state approximation, since **2** was not detected in either stoichiometric reactions or catalysis. The resulting rate law is more complex. When assuming the $[CO_2]$ is low, however, the simplified rate law is the same as in Scheme 5.

[32] ATH of acp becomes significantly slower at pH $>$ 10. Also see reference [5i].

[33] a) R. Noyori, M. Koizumi, D. Ishii, T. Ohkuma, *Pure Appl. Chem.* **2001**, *73*, 227; b) R. Noyori, M. Kitamura, T. Ohkuma, *Proc. Natl. Acad. Sci. USA* **2004**, *101*, 5356.

[34] a) C. P. Casey, J. B. Johnson, *J. Am. Chem. Soc.* **2005**, *127*, 1883; b) C. P. Casey, J. B. Johnson, S. W. Singer, Q. Cui, *J. Am. Chem. Soc.* **2005**, *127*, 3100; c) C. P. Casey, N. A. Strotman, S. E. Beetner, J. B. Johnson, D. C. Priebe, I. A. Guzei, *Organometallics* **2006**, *25*, 1236.

[35] a) D. A. Alonso, P. Brandt, S. J. M. Nordin, P. G. Andersson, *J. Am. Chem. Soc.* **1999**, *121*, 9580; b) J. W. Handgraaf, J. N. H. Reek, E. J. Meijer, *Organometallics* **2003**, *22*, 3150.

[36] In order to obtain a guess structure for **TS-C**, typical NH···O_{water} and H_{water}···O(=C) distances encountered in a H-bonding were chosen. Using a "Lock atoms, Modify & Optimise, Unlock" approach, we obtained a candidate structure for **TS-C**. The guess structure was optimised using the Eigenvector Following Method (J. Baker, *J. Comput. Chem.* **1986**, *7*, 385). However, the resulting structure was not a saddle point, as its vibrational spectrum was characterised with two negative frequencies (−73.6 and −39.1 cm^{-1}), thus excluding the structure to be a transition state for the reduction under question.

[37] Y. Zhao, J. Z. Pu, B. J. Lynch, D. G. Truhlar, *Phys. Chem. Chem. Phys.* **2004**, *6*, 673.

[38] a) T. Ohkuma, K. Tsutsumi, N. Utsumi, N. Arai, R. Noyori, K. Murata, *Org. Lett.* **2007**, *9*, 255; b) T. Ohkuma, N. Utsumi, M. Watanabe, K. Tsutsumi, N. Arai, K. Murata, *Org. Lett.* **2007**, *9*, 2565.

[39] N. Makihara, S. Ogo, Y. Watanabe, *Organometallics* **2001**, *20*, 497.

[40] A. B. Chaplin, C. Fellay, G. Laurenczy, P. J. Dyson, *Organometallics* **2007**, *26*, 586.

[41] This is confirmed by the reaction of triflic acid and DPPE under otherwise identical conditions. When an excess amount of triflic acid was added to a CD_2Cl_2 solution of DPPE, a sharp singlet at 10 ppm was observed. Broad singlets at $\delta = 9.2$ and −13.0 ppm were observed when excess DPPE present in solution.

[42] a) H. B. Zhang, L. Liu, Y. J. Chen, D. Wang, C. J. Li, *Eur. J. Org. Chem.* **2006**, 869; b) L. Chen, C. J. Li, *Adv. Synth. Catal.* **2006**, *348*, 1459; c) S. H. Cho, S. B. Chang, *Angew. Chem.* **2007**, *119*, 1929; *Angew. Chem. Int. Ed.* **2007**, *46*, 1897; d) S. Shirakawa, S. Kobayashi, *Synlett* **2006**, 1410; e) R. N. Butler, W. J. Cunningham, A. G. Coyne, L. A. Burke, *J. Am. Chem. Soc.* **2004**, *126*, 11923; f) D. G. Blackmond, A. Armstrong, V. Coombe, A. Wells, *Angew. Chem.* **2007**, *119*, 3872; *Angew. Chem. Int. Ed.* **2007**, *46*, 3798; g) C. Q. Yin, Z. T. Xu, S. Y. Yang, S. M. Ng, K. Y. Wong, Z. Y. Lin, C. P. Lau, *Organometallics* **2001**, *20*, 1216.

[43] a) J. Engberts, *Pure Appl. Chem.* **1995**, *67*, 823; b) G. K. vanderWel, J. W. Wijnen, J. Engberts, *J. Org. Chem.* **1996**, *61*, 9001; c) W. Blokzijl, J. Engberts, in *Structure and Reactivity in Aqueous Solution, Vol. 568*, ACS, Washington, **1994**, p. 303–317; d) G. I. Almerindo, J. R. Pliego, *Chem. Phys. Lett.* **2006**, *423*, 459.

[44] a) Y. Y. Ohnishi, Y. Nakao, H. Sato, S. Sakaki, *Organometallics* **2006**, *25*, 3352; b) H. Hayashi, S. Ogo, S. Fukuzumi, *Chem. Commun.* **2004**, 2714; c) G. Kovacs, G. Schubert, F. Joo, I. Papai, *Catal. Today* **2006**, *115*, 53; d) Y. Himeda, N. Onozawa-Komatsuzaki, H. Sugihara, K. Kasuga, *Organometallics* **2007**, *26*, 702.

[45] S. Arita, T. Koike, Y. Kayaki, T. Ikariya, *Angew. Chem.* **2008**, *120*, 2481; *Angew. Chem. Int. Ed.* **2008**, *47*, 2447.

[46] S. Ogo, H. Nakai, Y. Watanabe, *J. Am. Chem. Soc.* **2002**, *124*, 597.

[47] R. J. Hamilton, S. H. Bergens, *J. Am. Chem. Soc.* **2006**, *128*, 13700.

[48] a) B. Delley, *J. Chem. Phys.* **1990**, *92*, 508; b) B. Delley, *J. Chem. Phys.* **2000**, *113*, 7756; c) $DMol^3$, Material Studio version 3.2 from Accelerys: http://www.accelrys.com/products/mstudio/.

[49] a) A. D. Becke, *Phys. Rev. A* **1988**, *38*, 3098; b) C. T. Lee, W. T. Yang, R. G. Parr, *Phys. Rev. B* **1988**, *37*, 785.

[50] D. Di Tommaso, S. A. French, C. R. A. Catlow, *THEOCHEM* **2007**, *812*, 39.

[51] GAMESS-UK is a package of *ab initio* programs, see: http://www.cfs.dl.ac.uk/gamess-uk/index.shtml; M. F. Guest, I. J. Bush, H. J. J. van Dam, P. Sherwood, J. M. H. Thomas, J. H. van Lenthe, R. W. A. Havenith, K. Kendrick, "The GAMESS-UK electronic structure package: algorithms, developments and applications", *Mol. Phys.* **2005**, *103*, 719.

[52] Y. Zhao, B. J. Lynch, D. G. Truhlar, *J. Phys. Chem. A* **2004**, *108*, 2715.

[53] A. W. Ehlers, M. Bohme, S. Dapprich, A. Gobbi, A. Hollwarth, V. Jonas, K. F. Kohler, R. Stegmann, A. Veldkamp, G. Frenking, *Chem. Phys. Lett.* **1993**, *208*, 111.

Received: March 26, 2008
Published online: July 4, 2008

